Control of cell adhesion and detachment using temperature and thermoresponsive copolymer grafted culture surfaces

Yukiko Tsuda,[1,3] Akihiko Kikuchi,[2,3] Masayuki Yamato,[2,3] Yasuhisa Sakurai,[1] Mitsuo Umezu,[1] Teruo Okano[2,3]

[1]Graduate School of Science and Engineering, Waseda University, 3-4-1 Okubo, Shinjuku, Tokyo 169-8555, Japan
[2]Institute of Advanced Biomedical Engineering and Science, Tokyo Women's Medical University, 8-1 Kawada-cho, Shinjuku, Tokyo 162-8666, Japan
[3]Core Research for Evolutional Science and Technology, Japan Science and Technology Agency

Abstract: The hydrophobic monomer, n-butyl methacrylate (BMA) has been incorporated into thermoresponsive poly(N-isopropylacrylamide) (PIPAAm) to lower PIPAAm phase transition temperatures necessary for systematically regulating cell adhesion on and detachment from culture dishes at controlled temperatures. Poly(IPAAm-co-BMA)-grafted dishes were prepared by electron beam irradiation methods, systematically changing BMA content in the feed. Copolymer-grafted surfaces decreased grafted polymer transition temperatures with increasing BMA content as shown by water wettabilities compared to homopolymer PIPAAm-grafted surfaces. Bovine endothelial cells readily adhered and proliferated on copolymer-grafted surfaces above collapse temperature at 37°C, finally reaching confluence. Cell sheet detachment behavior from copolymer-grafted surfaces depended on the culture temperature and BMA content. In conclusion, cell attachment/detachment can be controlled to an arbitrary temperature by varying the content of hydrophobic monomer incorporated into PIPAAm grafted to culture surfaces. © 2004 Wiley Periodicals, Inc. J Biomed Mater Res 69A: 70–78, 2004

Key words: temperature responsive surfaces; poly(N-isopropylacrylamide); n-butyl methacrylate; copolymer grafting; cell culture; cell sheet

INTRODUCTION

Poly(N-isopropylacrylamide) (PIPAAm), a thermoresponsive polymer, has a lower critical solution temperature (LCST) at 32°C in aqueous solution.[1,2] PIPAAm is fully hydrated with an extended chain conformation below 32°C and is extensively dehydrated to become compact above 32°C. Because of its unique, reversible hydrophilic/hydrophobic property changes with temperature, many studies utilizing PIPAAm for various applications are reported, including temperature-controlled release as drug delivery systems,[2–4] aqueous chromatography systems for separations of bioactive compounds,[5–8] and bioconjugates to regulate enzymatic activities with tempera-

ture.[9–12] Additionally, we have extensively investigated the modulation of cultured cell adhesion and detachment on PIPAAm-grafted surfaces prepared by electron beam polymerization methods.[13–16] Because PIPAAm-grafted surfaces show reversible hydrophilic/hydrophobic property alterations with temperature, a variety of cells readily adhere to and proliferate on these modified surfaces dehydrated at 37°C but not to their hydrated surfaces below PIPAAm's transition temperature. Reducing cell culture temperature below 32°C permits enzyme-free recovery of confluent cultures of many cell types as a tissue-like single cell sheet maintaining cell–cell interactions and intact extracellular matrix (ECM) proteins on the cell sheet basal surfaces.[17] Thus, this thermal system is very effective for recovering adherent cells with minimal cell damage. Recovered cell sheets can be transferred and adhered onto other surfaces by using support transfer membranes.[18,19] These novel techniques represent a new method for reconstructing complex cell strata, pseudotissue, or organ-mimicking layered constructs in tissue engineering by overlaying recovered cell sheets.[20,21]

We also reported that successful coculture of two cell types using patterned grafting of PIPAAm onto TCPS dishes.[22,23] Culture surfaces with both thermo-responsive PIPAAm islands and thermally inert TCPS matrix seeded with hepatocytes and bovine aortic endothelial cells (BAECs) or human fetal lung fibro-blasts, TIG-1 on patterned surfaces exhibit coexisting cell-dependent functional increases, which now compels us to produce improved patterned, dual thermo-responsive polymers modified surfaces for coculture. Thus, the entire surface must be covered with thermo-responsive polymers of at least two different types, adding the required different transition temperatures. IPAAm copolymerized with other hydrophilic or hydrophobic monomers permits access to copolymers with widely varied transition temperatures.[2,24–26] By modifying surfaces with these copolymers having different transition temperatures, coculture of multiple cell types and recovery of functioning cocultured cell sheets should become possible with independent temperature alteration of the hydrophobicity of each respective patterned polymer domain on binary thermo-responsive surfaces.

In the present article, we describe cell attachment/detachment control with temperature-induced alteration of surface properties with grafted copolymers. To control cell attachment/detachment on tissue culture substrates at definite temperatures, IPAAm is copolymerized with hydrophobic monomer, BMA, and grafted to TCPS surfaces by electron beam irradiation. Surface hydration, and therefore cell attachment/detachment, are shown to be controlled to arbitrary temperatures using surface-grafted copolymers varying in incorporated BMA content.

MATERIALS AND METHODS

Materials

Commercial materials used in the modification of cell culture dishes were: IPAAm, generously provided by Kohjin (Tokyo, Japan) was purified by recrystallization from n-hexane and dried at 25°C under vacuum; n-butyl methacrylate (BMA) from Tokyo Chemical Industries Inc. (Tokyo, Japan) was distilled under reduced pressure and the fraction boiling at 80°C/L mmHg was used; and 2-propanol was obtained as high performance liquid chromatography grade from Kanto Chemical Co., Inc. (Tokyo, Japan) and used as received.

Tissue culture grade polystyrene dishes (TCPS, Falcon 3001and 3002) were obtained from Becton Dickinson Labware (Oxnard, CA). Dulbecco's modified Eagle's medium (DMEM) and Ca^{2+}-, and Mg^{2+}-free Dulbecco's phosphate-buffered saline (PBS) from Sigma Chemical Co. (St Louis, MO); and fetal bovine serum (FBS) from Moregate Exports Pty. Ltd. (Bulimba, QLD, Australia). Penicillin, streptomycin

as antibiotics, and trypsin-EDTA solution were obtained from Gibco Laboratories (Grand Island, NY). Bovine aortic endothelial cells (BAECs; lot No. HH JCRB0099) were obtained from Japan Health Science Foundation (Osaka, Japan). Cells were subcultured at a 1:4 ratio once a week and used between the 15th–25th passages to maintain characteristic cell functions.

Preparation of PIPAAm-grafted surfaces

PIPAAm-grafted cell culture surfaces were prepared as described elsewhere.[13] Briefly, a fixed amount of 55 w/w % IPAAm solution in 2-propanol was added and homogeneously spread to each TCPS dish and immediately irradiated with a 0.3 MGy electron beam (EB) (150 kV, under 10^{-5} Torr) using an area beam electron processing system (Nissin-High Voltage Co., Ltd., Kyoto, Japan) to polymerize and graft PIPAAm.[13] The PIPAAm-grafted dishes were extensively rinsed with cold distilled water to remove unreacted IPAAm and un-grafted PIPAAm, then thoroughly dried at 25°C under vacuum.

Preparation of poly (IPAAm-co-BMA)-grafted surfaces

Poly(IPAAm-co-BMA)-grafted surfaces were prepared by analogous electron beam polymerization. IPAAm and BMA mixed monomer solutions in 2-propanol were spread on each TCPS dish and then irradiated with the EB with identical conditions as described above. IB-grafted dishes were first washed with cold distilled water to remove unreacted IPAAm and ungrafted copolymers, then immersed in methanol for 1 day to remove unreacted BMA. These dishes were finally dried at 25°C under reduced pressure. Prepared copolymer dishes were encoded as IBX, where X denotes the mole fraction of BMA in feed.

Quantification of grafted polymers on TCPS surfaces

The amount of PIPAAm and IBX-grafted on the base TCPS dish surfaces was determined from infrared (IR) spectra using an attenuated total reflection-Fourier transform infrared spectrophotometer (ATR-FTIR, Valor-III equipped with an ATR-500M attachment, JASCO, Tokyo, Japan). Three samples each of PIPAAm-grafted and copolymer-grafted dishes were cut to 3 × 1 cm with an ultrasonic cutter (SUW30, Suzuki Motor Co., Shizuoka, Japan). Polystyrene as a base material of the modified surfaces has a strong absorption band attributed to monosubstituted aromatic rings at 1600 cm^{-1}. An absorption for amide carbonyl (amide I) of PIPAAm appears in the region of 1650 cm^{-1}.[18] The peak intensity ratio ($I_{1650/1600}$) was used to determine the amount of PIPAAm or copolymer grafted onto each surface using a calibration curve prepared for a known PIPAAm amount cast on TCPS dishes. An absorption band attributed to an

ester carbonyl of BMA appears at 1750 cm^{-1}. However, no strong absorption was acquired in this region for IB-grafted surfaces, probably due to the minute amounts of BMA incorporated. Consequently, the amount of copolymer grafted onto TCPS dishes was correlated to the identical amount of PIPAAm in the present research.

Static water contact angle measurements

Three samples each of PIPAAm-grafted, copolymer-grafted, and control TCPS dishes were cut to 3 × 1 cm to measure static water contact angles determined by the sessile drop method from 8 to 37°C with a FACE contact angle meter (Image processing type CA-X, Kyowa Interface Science, Saitama, Japan). MilliQ water was gently placed on the sample surfaces using a syringe. The contact angles were then measured after 30 s. All samples were measured more than five times and averaged.

Cell culture

Prepared dishes for cell culture use were sterilized with ethylene oxide gas. BAECs were cultured on TCPS dishes (Falcon 3002) containing 5 mL of DMEM supplemented with 10% FBS, 100 units/mL penicillin and 100 μg/mL streptomycin at 37°C under a humidified atmosphere with 5% CO_2 and 95% air. BAECs in confluent cultures were harvested from TCPS dishes by treatment with 0.5 mL of 0.25% trypsin–0.26 mM EDTA in PBS for 5 min and then diluted with 5 mL of DMEM to terminate enzymatic reactions. The recovered cell suspension was centrifuged at 800 rpm for 5 min with a centrifuge (RLX-105; TOMY, Tokyo, Japan) and resuspended in DMEM supplemented with 10% FBS prior to plating on grafted dishes. Cell morphology was monitored under a phase-contrast microscope (Eclipse TE300; Nikon, Tokyo, Japan) equipped with a digital camera (FinePix S1Pro, Fujifilm, Tokyo, Japan).

Temperature-dependent single cell adhesion

BAECs were seeded onto grafted PIPAAm- and IB5-grafted surfaces at a cell density of 1.0 × 10^4 cells/cm^2 and cultured with DMEM in the presence of 10% FBS at either 37 or 28°C. Morphologies of cultured cells were observed 24 h after seeding by phase-contrast microscopy.

Single cell detachment by low temperature treatment

BAECs were seeded onto grafted PIPAAm-, IB5-grafted, and control TCPS surfaces at a cell density of 1.0 × 10^4 cells/cm^2 and cultured with DMEM in the presence of 10% FBS at 37°C for 48 h. Nonadherent cells were removed by changing culture medium, then culture dishes were transferred to a CO_2 incubator set at 20°C. Remaining adherent cell numbers on each surface were counted periodically by acquiring phase contrast photographs.

Cell sheet recovery

BAECs were plated to grafted PIPAAm, IBX-grafted, and control TCPS surfaces at a cell density of 1 × 10^5 cells/cm^2 and cultured at 37°C. Culture medium was changed 24 h after seeding to remove nonadherent cells. After cells formed confluent monolayers on these surfaces, each plate was transferred to a CO_2 incubator set at either 28, 25, or 20°C and morphologies of cell monolayers were monitored periodically by acquiring phase contrast photographs. Areas of remaining adherent cells were measured using NIH Image (version 1.61) for the Macintosh. The area of remaining adherent cell sheets relative to in situ confluently cultured cell area was calculated and averaged.

RESULTS AND DISCUSSION

Surface characterization

PIPAAm and IBX were covalently immobilized to TCPS dishes by electron beam irradiation methods well described in the previous works.[13-23] In our previous report,[16] the amount of grafted PIPAAm onto TCPS dishes was known to influence thermal regulation of cell adhesion and lifting behavior. On PIPAAm-grafted surfaces with small amounts of PIPAAm (less than 1.5 μg/cm^2), cells adhere and proliferate as those on TCPS. However, they remain adherent and no cell lifting occurs even at 20°C, probably because grafted polymer hydration and subsequent surface property alterations are not sufficient to produce cell detachment at this low density. On the other hand, cells do not show either adhesion or proliferation on surfaces grafted with more than 2 μg/cm^2 of PIPAAm. In a preliminary experiment, IB3-grafted dishes were prepared with various concentration of IB monomer solution to control grafted amounts of copolymers and thus promote adequate cell adhesion/detachment with temperature alteration. Table I summarizes amounts of IB3 grafted to TCPS surfaces prepared from different monomer concentrations as determined by ATR-FTIR. Amounts of grafted polymer exceeded 2.3 μg/cm^2 at 40 and 50 w/w % feed, which is larger than that measured for PIPAAm-grafted surfaces. As expected, cell adhesion and proliferation were not observed on such surfaces grafted with more than 2.3 μg/cm^2 of polymer despite the presence of hydrophobic component, BMA [Fig. 1(d)]. However, endothelial cells adhered on IB3 surfaces

TABLE I
Grafted PIPAAm Densities as a Function
of Monomer Feed Concentration

Concentration of IB3-Monomer Solution (w/w %)	Amount of Grafted PIPAAm[a] ($\mu g/cm^2$)
30	2.01 ± 0.11
40	2.34 ± 0.12
50	2.36 ± 0.06

[a]Data are expressed as the mean of three samples with standard error of mean.

grafted with 2.01 $\mu g/cm^2$ prepared from 30 w/w % of monomer solution similar to that observed on both ungrafted TCPS and PIPAAm-grafted surfaces [Fig. 1(c)]. Therefore, in following experiments, concentration of IB-monomer feed solution was fixed to 30 w/w % during electron beam irradiation to homogeneously graft similar amounts of these copolymers to TCPS dishes. Table II summarizes the amounts of PIPAAm and IB-grafted to TCPS surfaces as determined by ATR-FTIR. All prepared surfaces were grafted with approximately 2 $\mu g/cm^2$ of PIPAAm or IBX. As will be described in the cell culture section, all of these prepared surfaces showed reliable and reproducible cell adhesion and proliferation at 37°C under culture conditions.

Surface wettability changes with temperature

Surface wettability is often correlated to cell adhesive behavior on surfaces, often showing optimal values.[27-30] Temperature-dependent wettability changes of PIPAAm- and IBX-grafted surfaces were therefore investigated. Temperature variation of static contact angles for polymer-grafted surfaces was determined using the sessile drop method at temperatures ranging from 8 to 37°C; data are shown in Figure 2. All prepared surfaces were thermoresponsive: they exhibit hydrophilicity at lower temperatures and become relatively hydrophobic at higher temperature ranges. Water contact angles of the PIPAAm-grafted surfaces demonstrate relatively large hydrophilic to hydrophobic changes with small temperature increases near 32°C.[31,32] Predictably from previous copolymer solution work,[6,24-26] IBX-grafted surfaces show decreasing wettability transition temperatures with increasing BMA content in the IB copolymer compared to homopolymer PIPAAm-grafted surfaces. Distinct temperature-dependent wettability changes were observed for all IB-grafted surfaces. However, the magnitude of hydrophilic to hydrophobic changes became smaller for the copolymer surfaces with increasing BMA content. These changes originate from known solution property alterations with temperature

for IB copolymers in aqueous condition.[6,24] As BMA content in the copolymer increases, hydrophobic BMA molecules interrupt the IPAAm chain sequence continuities required for cooperative transition, disrupting
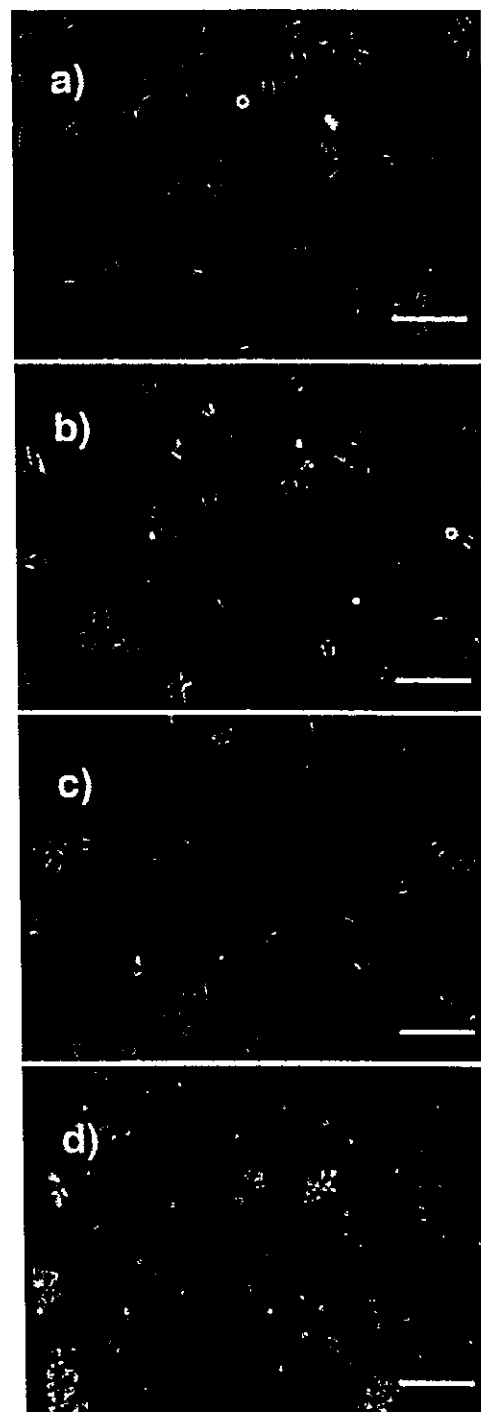

Figure 1. Cell morphologies on different IB3-grafted surfaces as a function of graft density. Grafted polymer densities measured by ATR-FTIR are: (a) 0; (b) 1.79 ± 0.01; (c) 2.01 ± 0.11; (d) 2.36 ± 0.06 $\mu g/cm^2$, respectively.

TABLE II
Grafted Polymer Densities on Prepared Surfaces
Determined by ATR-FTIR

Surface	Amount of Grafted PIPAAm[a] $(\mu g/cm^2)$
PIPAAm	1.79 ± 0.01
IB1	1.80 ± 0.04
IB3	2.01 ± 0.11
IB5	2.00 ± 0.02

[a]Data are expressed as the mean of three samples with standard error of mean.

segmental cooperative effects in temperature-dependent dehydration upon temperature increases. This produces a decreased temperature sensitivity with increasing BMA composition in IB grafted copolymers. Because BMA domains in grafted IB-copolymers are hydrophobic with solubility roughly independent of temperature changes, cooperative hydration of IPAAm components in the vicinity of BMA components are suppressed. Namely, inherent meta-stability of hydration around IB-copolymers induces dehydration of IPAAm side chains with only slight temperature increases. Additionally, each hydrophobic BMA domain produces hydrophobic interactions that induce chain aggregation of BMA components. Results of temperature-dependent wettability measurements on prepared surfaces show that transition temperatures observed for grafted copolymers on TCPS dishes
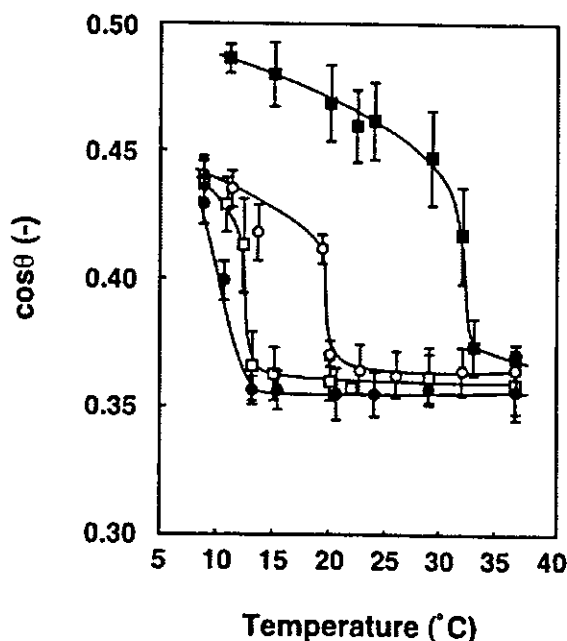

Figure 2. Temperature-dependent water contact angle changes for PIPAAm and IBX-grafted surfaces determined by sessile drop methods. Filled square, PIPAAm; open circle, IB1; open square, IB3; filled circle, IB5.
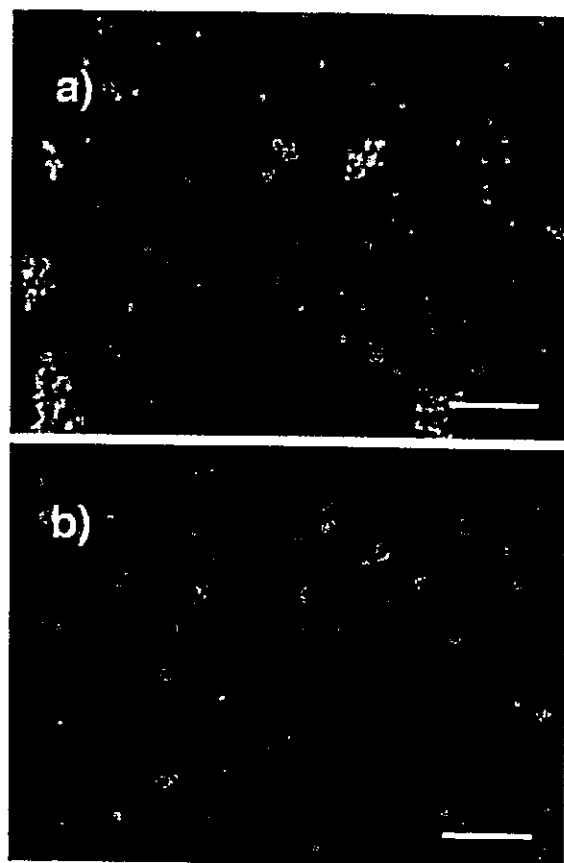

Figure 3. Microscopic views of BAECs seeded on (a) PIPAAm- and (b) IB5-grafted surfaces after 24-h culture in serum-containing media at 28°C. Scale bar: 100 μm.

are correlated to the amount of incorporated hydrophobic BMA.

Temperature-dependent single cell adhesion

Temperature-dependent cell adhesion to PIPAAm- and IB5-grafted surfaces was investigated. BAECs were sparsely seeded on prepared dishes and cultured at 28 or 37°C for 24 h in DMEM with 10% FBS. After 24-h incubation at 37°C, BAECs readily adhered and spread well on both PIPAAm- and IB5-grafted surfaces (data not shown). These results correlate with surface wettability data that both surfaces are hydrophobic at this temperature. Adherent cell numbers and morphologies were identical between PIPAAm- and IB5-grafted surfaces. By contrast, at 28°C, slightly below the transition temperature for PIPAAm, no seeded cells adhered onto PIPAAm-grafted surfaces because PIPAAm was sufficiently hydrated to suppress cell adhesion [Fig.3(a)]. Additionally, seeded cells adhered and became well spread on IB5-grafted
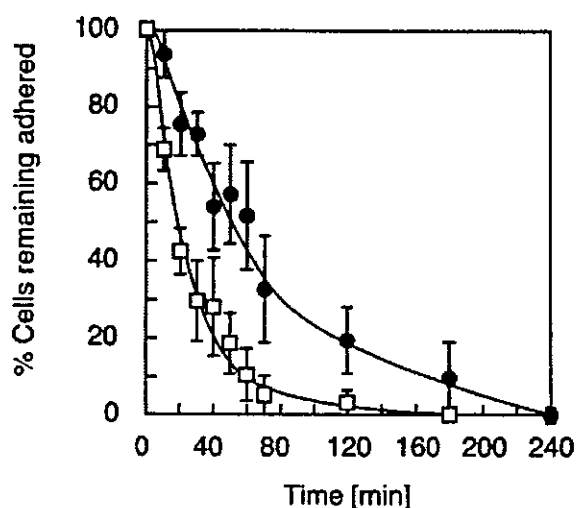
Figure 4. Time-dependent cell detachment from PIPAAm- and IB5-grafted surfaces by low temperature treatment at 20°C after 48-h culture at 37°C. Data are expressed as the mean with standard error of mean ($n = 3$). Initial seeded cell density: 1×10^4 cells/cm^2. Open square, PIPAAm; filled circle, IB5.

surfaces [Fig.3(b)]. Hydrophobic BMA components suppressed PIPAAm hydration at this temperature, promoting cell adhesion on IB5-grafted surfaces. This indicated that culture temperatures promoting cell adhesion could be reduced and regulated by copolymerizing with the hydrophobic monomer, BMA.

Single-cell detachment by low temperature treatments

After 48-h culture at 37°C, seeded BAECs adhered well and showed spread morphologies on both PIPAAm- and IB5-grafted surfaces. Cell adhesion on those dishes was nearly identical with that on TCPS dishes (data not shown). Culture temperature was then reduced to 20°C and cell detachment from the PIPAAm- and IB5-grafted dishes were observed. No cell detachment was observed from TCPS surfaces within the examined time ranges up to 24 h. Figure 4 shows time dependence for cells remaining adherent on surfaces. In detachment, individual cells spontaneously changed their shape from a spread to a round form without any enzymatic treatment, and finally cultured cells detached completely from both PIPAAm- and IB5-grafted surfaces. A majority of cells (ca. 90%) detached within 1 h, then, 3 h after incubation at 20°C, all cells were detached from PIPAAm-grafted dishes. However, another 1-h incubation was required for complete cell detachment from IB5-grafted dishes because hydrophobic BMA molecules in the copolymer reduce the copolymer hydrophilicity

to reduce surface hydration and resulting cell lifting. These results clearly demonstrate that the grafted polymer hydration significantly influences cell–materials interaction, namely, more hydrophobic surfaces decelerate cell lifting. A discrepancy between surface wettability and cell detachment from IB5-grafted surfaces can be seen by comparing data in Figures 2 and 4. Namely, cells detached even though IB-5 surfaces remain hydrophobic state at 20°C from the data in Figure 2. In cell detachment experiments, polymer-grafted surfaces were always exposed to aqueous medium at 37°C during cell adhesion. By contrast, contact angles were measured on dry polymer-grafted surface samples. Such differences may influence the observed discrepancy. By lowering temperature, IPAAm sequences in surface grafted IB5 chains become hydration, although the degree is small as hydrophobic BMA units suppress complete hydration as was seen for PIPAAm-grafted surfaces. Such a hydration on IPAAm sequences may effect to cell detachment process from IB5-grafted surfaces upon reducing temperature to 20°C.[33] Cell attachment and detachment are thus controllable by regulating BMA content in the grafted copolymers.

Cell sheet detachment from grafted surfaces

In our previous reports,[17,19] enzyme-free harvest of confluently cultured cell monolayers was achieved in tissue-like cell sheets by only lowering culture temperatures to 20°C, altering surface properties to hydrophilic. Here, temperature-dependent spontaneous cell sheet detachment was investigated on copolymer grafted surfaces to examine influences of copolymer composition. Seeded BAECs on PIPAAm, IBX-grafted, and control TCPS surfaces readily adhered and proliferated in serum media, reaching confluence with cell–cell junction formation at 37°C without precoating of adhesive ECM proteins. Cell adhesion and spreading on these surfaces 4 days after seeding were identical in both morphologies and cell densities. These dishes were then transferred into CO$_2$ incubators adjusted either to 28, 25, or 20°C. Cell monolayer sheet detachment processes from both PIPAAm- and IB5-grafted surfaces were photographed over time and shown in Figure 5. Detachment was basically similar for all grafted surfaces as indicated in Figure 5 and reported previously.[17-21] First, cultured cell monolayers start detaching spontaneously from the edges of (co)polymer-grafted surfaces [Fig. 5(b) and (e)] accompanying the surface property alteration. Then cell sheets gradually lift off with accompanying sheet shrinkage and agglomeration. They finally completely detach as a single piece from the modified surfaces and float in the medium [Fig. 5(c) and (f)].
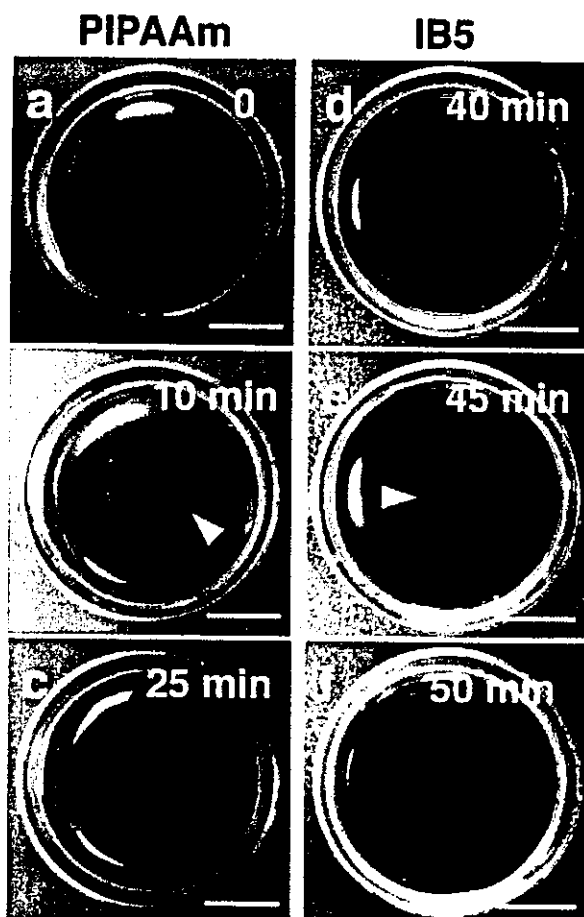
PIPAAm　　　IB5

Figure 5. Macroscopic view of time-dependent detachment of confluent cultures of endothelial cells from PIPAAm-grafted (a–c) and IB5-grafted (d–f) surfaces at 20°C, showing both detached and adherent portions of BAEC monolayers. PIPAAm-grafted surface: (a) 0; (b) 10; and (c) 25 min, IB5-grafted surface: (d) 40; and (e) 45; and (f) 50 min after incubation at 20°C. Scale bar = 1 cm.

Contraction of recovered cell sheets is probably due to the disappearance of anchorage-dependence caused by surface hydration, and to the strong cell–cell interactions within the sheet. From the photographs acquired during detachment processes at different temperatures, areal changes in cells remaining adherent on these thermoresponsive surfaces were digitized on NIH Image software over time.

Figure 6 shows time-dependent areal changes of cell monolayers for thermoresponsive surfaces at three low-temperature conditions. Cells on control TCPS surfaces remain adherent regardless of temperature and time (data not shown). It is clear that recovery of cell sheets and time required for complete sheet detachment are closely related to the composition of surface-grafted polymers and treatment temperatures. At any treatment temperature, longer incubation times were required to complete cell detachment with

increasing BMA content in the copolymers. Cell sheet detachment was accelerated by reducing temperature from 28 to 20°C. At 28°C, detachment of cell monolayers was observed from only PIPAAm- and IB1-grafted surfaces, while no cell monolayers detached from either IB3- and IB5-grafted surfaces within the examined time ranges to 24 h. IB3- and IB5-grafted surfaces remained hydrophobic at this temperature, allowing cells to remain adhered on the modified surfaces. In sharp contrast, PIPAAm- and IB1-grafted surfaces became hydrophilic through hydration of grafted polymer molecules, promoting cell detachment from the hydrated surfaces at 28°C. Further low-temperature treatment at 25 and 20°C allows accelerated cell sheet detachment from all surface types. Complete cell sheet detachment occurred from IB1-grafted surfaces after 60-min incubation at 28°C, while only 30-min incubation is necessary at 20°C. Similarly, while cell sheets remained adherent on IB5-grafted surfaces at 28°C, they were completely recovered in 150 min at 25°C and in 50 min at 20°C, respectively.
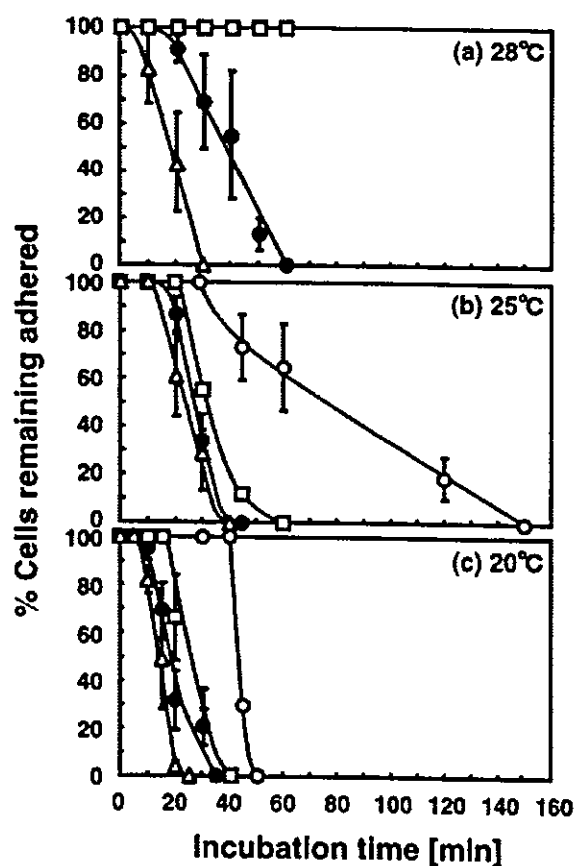

Figure 6. Time-dependent cell sheet area remaining adherent on PIPAAm-, and IBX-grafted surfaces: Open triangle, PIPAAm; filled circle, IB1; open square, IB3; open circle, IB5 at various temperature: (a) 28°C; (b) 25°C; (c) 20°C. Data are expressed as the mean with standard error of mean (n = 3–5).

Cell sheet detachment process and required times for complete cell sheet detachment are dependent on modifier characteristics as well as temperature treated. Detachment rate was almost identical for all samples once cell detachment initiated from the periphery of cell monolayer at either 20 or 25°C except for IB5 at 25°C, although starting time for cell sheet detachment retarded with increasing BMA content in the copolymer. Hydration of surface grafted polymers may play crucial role at the beginning of cell sheet detachment, the more hydrophilic polymers were grafted on the surfaces, the faster initial cell detachment at the periphery was observed. Once cell sheet periphery detached, cell-to-cell interactions and contraction facilitate whole cell-sheet detachment. Therefore, almost identical detachment rate was observed regardless of polymer types.

With increasing BMA content in the copolymers, time required for cell sheet detachment was extended. Low-temperature treatment for longer time periods would deteriorate cellular metabolic functions. Kwon et al.[34] grafted PIPAAm onto porous membranes and succeeded in accelerating cultured cell monolayer detachment with low-temperature treatment by allowing rapid PIPAAm hydration through increased thermal and water transport. Higher cell-sheet detachment rates are therefore expected by grafting IBX onto porous membranes[34] and/or cografting with poly(ethylene glycol),[35] known also to promote rapid hydration and more dynamic polymer molecular motion. Furthermore, cell monolayers can be recovered without cell sheet aggolemeration and permitting transfer to other surfaces with hydrophilic poly(vinylidene difluoride) (PVDF) support membranes as reported in elsewhere.[19,20,36]

The present research reveals that cell detachment temperature can be modulated below 32°C by introducing BMA as the hydrophobic component to PIPAAm. Through a patterned grafting technique,[22,23] spatial cell arrangements with two cell types and thermal recovery can now be performed using spatial patterns grafting different thermoresponsive polymers. Such a strategy can be applied to construct more complicated tissues through cell sheet engineering technologies. Pattern coculture of two cell types on such patterned surfaces with different thermal responses will be presented in forthcoming separate technical reports.

CONCLUSIONS

A hydrophobic monomer, BMA, was incorporated into PIPAAm and grafted onto TCPS dishes by electron beam irradiation. Changes in BMA content in the copolymers resulted in regulation of both surface wet-

tability transition temperatures and the magnitude of wettability changes. These surface property alterations with BMA play important roles in cell adhesion/detachment control at various temperatures. The present surface modification technique should prove useful for recovery of two-dimensional cocultured cell sheets with surfaces pattern-grafted with PIPAAm and copolymers for tissue engineering applications, as well as basic research in cell-cell communication and coculture *in vitro*.

References

1. Heskins M, Guillent JE, James E. Solution properties of poly(N-isopropylacrylamide). J Macromol Sci Chem 1968;A2:1441–1445.
2. Bae YH, Okano T, Kim SW. Temperature dependence of swelling of crosslinked poly(N,N'-alkyl substituted acrylamides) in water. J Polym Sci Polym Phys 1990;28:923–936.
3. Bae YH, Okano T, Kim SW. "On–off" thermocontrol of solute transport I. Temperature dependence of swelling on N-isopropylacrylamide networks modified with hydrophilic components in water. Pharmaceut Res 1991;8:531–537.
4. Bae YH, Okano T, Kim SW. "On–off" thermocontrol of solute transport II. Solute release from thermosensitive hydrogels. Pharmaceut Res 1991;8:624–628.
5. Kanazawa H, Yamamoto K, Matsushima Y, Takai N, Kikuchi A, Sakurai Y, Okano T. Temperature-responsive chromatography using poly(N-isopropylacrylamide)-modified silica. Anal Chem 1996;68:100–105.
6. Kanazawa H, Kashiwase Y, Yamamoto K, Matsushima Y, Kikuchi A, Sakurai Y, Okano T. Temperature-responsive liquid chromatography. 2. Effects of hydrophobic groups in N-isopropylacrylamide copolymer-modified silica. Anal Chem 1997;69:823–830.
7. Kikuchi A, Okano T. Intelligent thermoresponsive polymeric stationary phase for aqueous chromatography of biological compounds. Prog Polym Sci 2002;27:1165–1193.
8. Malmstadt N, Yager P, Hoffman AS, Stayton PS. A smart microfluidic affinity chromatography matrix composed of poly(N-isopropylacrylamide)-coated beads. Anal Chem 2003; 75:2943–2949.
9. Stayton PS, Shimoboji T, Long C, Chilkoti A, Chen G, Harris JM, Hoffman AS. Control of protein-ligand recognition using a stimuli-responsive polymer. Nature 1995;378:472–474.
10. Matsukata M, Aoki T, Sanui K, Ogata N, Kikuchi A, Sakurai Y, Okano T. Effect of molecular architecture of poly(N-isopropylacrylamide)-trypsin conjugates on their solution and enzymatic properties. Bioconjugate Chem 1996;7:96–101.
11. Ding Z, Long CJ, Hayashi Y, Bulmus EV, Hoffman AS, Stayton PS. Temperature control of biotin binding and release with a streptavidin-poly(N-isopropylacrylamide) site-specific conjugate. Bioconjugate Chem 1999;10:395–400.
12. Hoffman AS, Stayton PS, Bulmus V, Chen G, Chen J, Cheung C, Chilkoti A, Ding Z, Dong L, Fong R, Lackey CA, Long CJ, Press OW, Shimoboji T, Shoemaker S, Yang HJ, Monji N, Nowinski RC, Cole CA, Priest JH, Harris JM, Nakamae K, Nishino T, Miyata T. Really smart bioconjugates of smart poly-

mers and receptor proteins. J Biomed Mater Res 2000;52:577–586.

13. Yamada N, Okano T, Sakai H, Karikusa F, Sawasaki Y, Sakurai Y. Thermo-responsive polymer surfaces; Control of attachment and detachment of cultured cells. Makromol Chem Rapid Commun 1990;11:571–576.

14. Okano T, Yamada N, Sakai H, Sakurai Y. A novel recovery system for cultured cells using plasma-treated polystyrene dishes grafted with poly(N-isopropylacrylamide). J Biomed Mater Res 1993;27:1243–1251.

15. Okano T, Yamada N, Okuhara M, Sakai H, Sakurai Y. Mechanisim of cell detachment from temperature-modulated, hydrophilic-hydrophobic polymer surfaces. Biomaterials 1995;16:297–303.

16. Sakai H, Doi Y, Okano T, Yamada N, Sakurai Y. Thermoresponsive polymer surfaces for cell culture: Analysis of the surfaces and control of the cell attachment/detachment. In Ogata N, SW Kim, Feijen J, Okano T, editors. Advanced biomaterials in biomedical engineering and drug delivery systems. Tokyo: Springer-Verlag; 1996. p 229–230.

17. Kushida A, Yamato M, Konno C, Kikuchi A, Sakurai Y, Okano T. Decrease in culture temperature releases monolayer endothelial cell sheets together with deposited fibronectin matrix from temperature-responsive culture surfaces. J Biomed Mater Res 1999;45:355–362.

18. Kikuchi A, Okuhara M, Karikusa F, Sakurai Y, Okano T. Two-dimensional manipulation of confluently cultured vascular endothelial cells using temperature-responsive poly(N-isopropylacrylamide)-grafted surfaces. J Biomater Sci Polym Ed 1998;9:1331–1348.

19. Hirose M, Kwon OH, Yamato M, Kikuchi A, Okano T. Creation of designed shape cell sheets that are noninvasively harvested and moved onto another surface. Biomacromolecules 2000;1:377–381.

20. Harimoto M, Yamato M, Hirose M, Takahashi C, Isoi Y, Kikuchi A, Okano T. Novel approach for achieving double-layered cell sheets co-culture: Overlayering endothelial cell sheets onto monolayer hepatocytes utilizing temperature-responsive culture dishes. J Biomed Mater Res 2002;62:464–470.

21. Shimizu T, Yamato M, Isoi Y, Akutsu T, Setomaru T, Abe K, Kikuchi A, Umezu M, Okano T. Fabrication of pulsatile cardiac tissue grafts using a novel 3-dimensional cell sheet manipulation technique and temperature-responsive cell culture surfaces. Circ Res 2002;90:e40–e48.

22. Yamato M, Kwon OH, Hirose M, Kikuchi A, Okano T. Novel patterned cell coculture utilizing thermally responsive grafted polymer surfaces. J Biomed Mater Res 2001;55:137–140.

23. Yamato M, Konno C, Utsumi M, Kikuchi A, Okano T. Thermally responsive polymer-grafted surfaces facilitate patterned cell seeding and co-culture. Biomaterials 2002;23:561–567.

24. Takei YG, Aoki T, Sanui K, Ogata N, Okano T, Sakurai Y. Temperature-responsive bioconjugates. 2. Molecular design for temperature-modulated bioseparations. Bioconjugate Chem 1993;4:341–346.

25. Iwata H, Oodate M, Uyama Y, Amemiya H, Ikada Y. Preparation of temperature-sensitive membranes by graft polymerization onto a porous membrane. J Membr Sci 1991;55:119–130.

26. Feil H, Bae YH, Feijen J, Kim SW. Effect of comonomer hydrophilicity and ionization on the lower critical solution temperature of N-isopropylacrylamide copolymers. Macromolecules 1993;26:2496–2500.

27. van Wachem PB, Beugeling T, Feijen J, Bantjes A, Detmers JP, van Aken WG. Interaction of cultured human endothelial cells with polymeric surfaces with different wettabilities. Biomaterials 1985;6:403–408.

28. van Wachem PB, Hogt AH, Beugeling T, Feijen J, Bantijes A, Detmers JP, van Aken WG. Adhesion of cultured human endothelial cells onto methacrylate polymers with varying surface wettability and charge. Biomaterials 1987;8:323–328.

29. Lee JH, Park JW, Lee HB. Cell adhesion and growth on polymer surfaces with hydroxyl groups prepared by water vapour plasma treatment. Biomaterials 1991;12:443–448.

30. Tamada Y, Ikada Y. Fibroblast growth on polymer surfaces and biosynthesis of collagen. J Biomed Mater Res 1994;28:783–789.

31. Takei YG, Aoki T, Sanui K, Ogata N, Sakurai Y, Okano T. Dynamic contact angle measurement of temperature-responsive surface properties for poly(N-isopropylacrylamide) grafted surfaces. Macromolecules 1994;27:6163–6166.

32. Yakushiji T, Sakai K, Kikuchi A, Aoyagi T, Sakurai Y, Okano T. Graft architectural effects on thermoresponsive wettability changes of poly(N-isopropylacrylamide)-modified surfaces. Langmuir 1998;14:4657–4662.

33. Dong L, Hoffman AS. A novel approach for preparation of pH-sensitive hydrogels for enteric drug delivery. J Controlled Release 1991;15:141–152.

34. Kwon OH, Kikuchi A, Yamato M, Sakurai Y, Okano T. Rapid cell sheet detachment from poly(N-isopropylacrylamide)-grafted porous cell culture membranes. J Biomed Mater Res 2000;50:82–89.

35. Kwon OH, Kikuchi A, Yamato M, Okano T. Accelerated cell sheet recovery by co-grafting of PEG with PIPAAm onto porous cell culture membranes. Biomaterials 2003;24:1223–1232.

36. Kushida A, Yamato M, Kikuchi A, Okano T. Two-dimensional manipulation of differentiated Madin-Darby canine kidney (MDCK) cell sheets: The noninvasive harvest from temperature-responsive culture dishes and transfer to other surfaces. J Biomed Mater Res 2001;54:37–46.

Temperature-Responsive Cell Culture Surfaces Enable "On−Off" Affinity Control between Cell Integrins and RGDS Ligands

Mitsuhiro Ebara,[†] Masayuki Yamato,[‡] Takao Aoyagi,[‡] Akihiko Kikuchi,[‡]
Kiyotaka Sakai,[†] and Teruo Okano*,[‡]

*Department of Applied Chemistry, Waseda University, 3-4-1 Ohkubo, Shinjuku-ku, Tokyo 169-8555, Japan,
and Institute of Advanced Biomedical Engineering and Science, Tokyo Women's Medical University,
8-1 Kawada-cho, Shinjuku-ku, Tokyo 162-8666, Japan*

In this study, specific interactions between immobilized RGDS (Arg-Gly-Asp-Ser) cell adhesion peptides and cell integrin receptors located on cell membranes are controlled in vitro using stimuli-responsive polymer surface chemistry. Temperature-responsive poly(N-isopropylacrylamide-co-2-carboxyisopropylacrylamide) (P(IPAAm-co-CIPAAm)) copolymer grafted onto tissue culture grade polystyrene (TCPS) dishes permits RGDS immobilization. These surfaces facilitate the spreading of human umbilical vein endothelial cells (HUVECs) without serum depending on RGDS surface content at 37 °C (above the lower critical solution temperature, LCST, of the copolymer). Moreover, cells spread on RGDS-immobilized surfaces at 37 °C detach spontaneously by lowering culture temperature below the LCST as hydrated grafted copolymer chains dissociate immobilized RGDS from cell integrins. These cell lifting behaviors upon hydration are similar to results using soluble RGDS in culture as a competitive substitution for immobilized ligands. Binding of cell integrins to immobilized RGDS on cell culture substrates can be reversed spontaneously using mild environmental stimulation, such as temperature, without enzymatic or chemical treatment. These findings are important for control of specific interactions between proteins and cells, and subsequent "on−off" regulation of their function. Furthermore, the method allows serum-free cell culture and trypsin-free cell harvest, essentially removing mammalian-sourced components from the culture process.

Introduction

Specific interactions between biomolecules and their molecular recognition play important roles in biology and physiology. Particularly, interactions between cell receptors and bioactive extracellular matrix proteins are necessary to maintain multiple cell functions. Appropriate chemical methodologies for biomaterial design that regulate bioactivities of proteins and cells are increasingly popular.[1−3] Particularly, control of specific interactions between bioactive molecules has been used to study, understand and control molecular recognition mediating biological process.[4,5] Recently, intelligent materials that exploit stimuli-responsive properties have demonstrated "on−off" control of various functional changes useful for biomedical applications.[6−8] Hoffman et al. have conjugated thermally responsive polymers with streptavidin near the biotin binding site to control the binding affinity of biotinylated proteins using a "polymer-shielding" effect.[9] They found that these "affinity switches" attributed to the degree of shielding depended on both the size of the biotinylated protein and the size of the grafted polymer. Moreover, we had previously shown regulation of

protein binding to surface-immobilized ligands using the spacer molecules and expanded coil/collapsed changes of co-immobilized temperature-responsive polymers.[10] Chromatographic analyses showed a clear correlation between spacer length and binding capacity by applying step temperature gradients.

The interaction of ligands and cell membrane receptors plays multiple important roles for inducing cell spreading, proliferation, differentiation, and signal transduction.[11−15] The extracellular matrix (ECM) elaborated by cells on surfaces constitutes a regulator of the cell adhesion process, cell differentiation, and contributes to the mechanical properties of tissue. These regulatory effects of ECM are mediated through transmembrane proteins specialized in cell−substrate adhesion. The peptide sequence Arg−Gly−Asp (RGD) found in fibronectin, type I collagen, and other extracellular matrix proteins has been widely studied as an immobilized cell adhesion ligand specific for integrin-mediated cell adhesion.[16,17] Surface density and chemical presentation of these synthetic ligands and their effectiveness as surface modification agents in cell culture is correlated to their ability to enhance cell adhesion, particularly, useful for applications in tissue engineering.[18−25]

In this study, we have designed the "on−off" switching study between cell integrins and the ligand peptide RGDS (Arg−Gly−Asp−Ser) in culture using noninvasive thermal

* To whom the correspondence should be addressed. E-mail: tokano@ abmes.twmu.ac.jp. Tel: +81-3-3353-8111 ext. 30233. Fax +81-3-3359-6046.
† Waseda University.
‡ Tokyo Women's Medical University.

control. Temperature responsive poly(N-isopropylacrylamide) (PIPAAm)-grafted surfaces are modified with RGDS peptides. Surface swelling, wettabilities, and modulus of the grafted surfaces can be changed by temperature control. Above the lower critical solution temperature (LCST) of PIPAAm, the grafted polymer chains collapse, and the immobilized peptide is therefore exposed to adherent cells. Below the LCST, hydrated polymer chains soften, expand, and swell, shielding immobilized RGDS from integrin access, limiting cell-surface attachment tension, and mechanically disrupting cell-surface contacts. Adherent cell populations are first rounded and then removed under this thermal treatment in the absence of serum proteins or trypsin treatment. The approach obviates the need for exogenous protein addition during culture and is useful for serum-sensitive or trypsin-sensitive cell types, particularly those useful for biomedical tissue engineered devices.

Experimental Section

Materials. N-Isopropylacrylamide (IPAAm) was kindly provided from Kojin Co. (Tokyo, Japan), and purified by recrystallization from n-hexane. 2-Carboxyisopropylacrylamide (CIPAAm) was synthesized as described previously.[26] Acrylic acid (AAc) was purchased from Wako Pure Chemicals Co., (Tokyo, Japan) and distilled under reduced pressure. Tissue culture grade polystylene (TCPS) dishes (Falcon 3001) were purchased from Becton Dickinson Labware (Oxnard, CA). Both RGDS (−Arg−Gly−Asp−Ser−) and RGES (−Arg−Gly−Glu−Ser−) linear peptides were purchased from Sigma (St. Louis, MO). 1-Ethyl-3-(3-dimethyl-aminopropyl)-carbodiimide hydrochloride (WSC) was purchased from Dojindo Laboratories (Kumamoto, Japan). Trypsin-EDTA solution, streptomycin, and penicillin were purchased from Gibco BRL (Grand Island, NY). Human umbilical vein endothelial cells (HUVECs), EBM-2 as their medium, and EGM-2 as supplements for medium were purchased from BioWhittaker (Walkersville, MD).

Preparation of Temperature-Responsive Polymer-Grafted Surfaces Modified with Peptides. PIPAAm-grafted surfaces were prepared as described previously.[27,28] Briefly, IPAAm and CIPAAm (used as carboxylate-terminated comonomer for peptide immobilization) were dissolved in 2-propanol at a total concentration of 55% (wt/wt) and 30 μL of the solution is spread uniformly over the surface of 35-mm TCPS dishes. These solutions contained different concentrations of CIPAAm comonomer (1−10 mol %) in the feed. Then, electron beam irradiation using an area beam electron processing system (Curetron EBC-200-AA2, Nissin High Voltage Co. Ltd., Kyoto, Japan) at a radiation dose of 0.3 MGy polymerizes and covalently grafts these monomers onto the TCPS surfaces. After rinsing and drying, 1 mL of Dulbecco's phosphate buffered saline (PBS; pH7.4) containing both RGDS (2 mM) and the same amount of WSC (2 mM) were spread over the surfaces at room temperature. The reacted peptide amount was large excessive to the surface carboxyl group content. Similarly RGES-immobilized surfaces, with the substitution of glutamic acid (E) for aspartic acid (D), were prepared to confirm the biospecificity

of the RGDS motif toward HUVEC integrins. Moreover, to compare different presentations of peptides via carboxylic comonomer immobilization, P(IPAAm-co-AAc)-grafted surfaces were also prepared and reacted with RGDS by identical methods. After 24 h, these dishes were rinsed with distilled water and sterilized with ethylene oxide after drying. These RGDS and RGES-immobilized P(IPAAm-co-CIPAAm)-grafted TCPS surfaces were abbreviated as RGDS−IC(X) and RGES−IC(X), respectively, and RGDS-immobilized P(IPAAm-co-AAc)-grafted TCPS surfaces was abbreviated as RGDS−IA(X), where X is the mole percent of carboxylated monomer in feed.

Cell Spreading Assay. HUVECs were cultured on TCPS dishes with EBM-2 supplemented with EGM-2 containing hFGF−B, VEGF, R3IGF-1, ascorbic acid, heparin, hEGF, hydrocortisone, gentamaicin/amphotericin-B (GA-1000) and fetal bovine serum (FBS) in humidified atmosphere with 5% CO_2. The cells were harvested from TCPS dishes with 0.25% trypsin−0.26 mM EDTA in phosphate buffered saline (PBS). Subcultures up to passage 3 were used for this study. EBM-2 supplemented with EGM-2 except for FBS was added, and the cells were centrifuged and resuspended in the serum-containing (2% FBS) or serum-free medium. A fixed number of cells (1.0×10^5 cells in 1 mL serum-free culture medium) were plated onto RGDS-immobilized PIPAAm-grafted surfaces and cultured in serum-free media at 37 °C in humidified atmosphere, 5% CO_2. Cell morphology was monitored and photographed under a phase contrast microscope (TE300, Nikon, Tokyo) after 6- and 24-h culture. In this study, "spread cell" are defined as well-adherent flat-shaped cell. The cell number was also counted from printed photographs and presented as mean ± standard deviation ($n = 3$).

Cell Detachment Assay. The lifting behavior of HUVECs from RGDS−IC(X) was investigated both by low-temperature treatment and soluble RGDS addition after indicated culture times without serum at 37 °C (4 h, 1 day, 3 days, and 7 days). For low-temperature treatment, spread cells were transferred to a CO_2 incubator equipped with a cooling unit fixed at 20 °C. For the competitive assay, soluble RGDS (100 μM) was added into culture dishes and incubated at 20 and 37 °C. The cell morphology was continuously observed and microphotographed under a phase contrast microscope. The percentage of spread cells to the initial spread cells was presented as a mean ± standard deviation ($n = 3$).

Results

Enhancement of Cell Spreading Mediated by Biospecific Interaction between Cell Integrins and Immobilized RGDS. To confirm the biospecificity of RGDS immobilized on grafted temperature-responsive polymers, HUVECs were seeded onto RGDS−IC(X) under serum-free conditions at 37 °C. The spread cell number after a 6-h culture increased depending on the co-monomer carboxylate group density on the surface, resulting from increasing RGDS immobilization probability to carboxyl groups on these surfaces (Figure 1).

Immobilized RGDS contributed to enhancement of cell spreading, likely mediated by cell integrins. By contrast, the control RGES-immobilized surfaces (RGES−IC(X)) did not
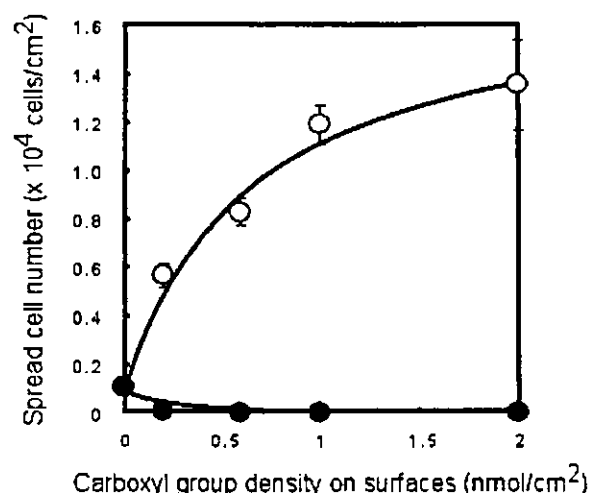
Figure 1. HUVEC spreading on RGDS and RGES-immobilized temperature-responsive culture surfaces after a 6-h culture without serum at 37 °C. These peptides were covalently grafted on P(IPAAm-co-CIPAAm)-grafted surfaces. The feed concentration of peptides was 2 mM. Symbols: RGDS−IC(X) (open circle) and RGES−IC(X) (closed circle).
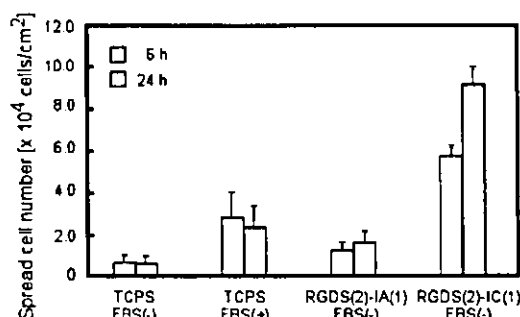
Figure 3. Phase-contrast photographs of HUVECs on temperature-responsive culture surfaces after a 6-h culture without serum at 37 °C before (a) and after (b) 2 mM of RGDS surface immobilization. Bar = 100 μm.

Figure 2. Comparisons of HUVEC spreading on various culture surfaces after 6- or 24-h cultures with or without serum at 37 °C. The surfaces used in this experiment were TCPS with/without serum, RGDS−IA(1) without serum, and RGDS−IC(1) without serum.

Figure 4. Competitive assay for HUVEC detachment from RGDS-immobilized temperature-responsive culture surfaces by soluble peptide addition. Soluble RGDS (100 μM) was added to cells on RGDS−IC(X) after a 24-h culture at 37 °C without serum. CIPAAm compositions were 1 (open circle), 3 (triangle), 5 (square), and 10 mol % (diamond). As a comparison, cells cultured on TCPS for 24 h at 37 °C with serum were detached at 20 °C (closed circle).

demonstrate cell spreading enhancement against immobilized peptides density because they have no integrin biospecificity with the substitution of glutamic acid (E) for aspartic acid (D).[29] Figure 2 shows spread HUVEC numbers on various substrates after 6-h and 24-h cultures with or without serum at 37 °C. Although addition of dilute serum facilitates HUVEC spreading on TCPS, RGDS−IC(1) promoted cell spreading dramatically under serum-free conditions. By contrast, spreading improvement was hardly observed on the RGDS−IA(1) surface where peptides are immobilized via another comonomer, AAc, in place of CIPAAm. As seen in Figure 3, significant differences in HUVEC spreading on P(IPAAm-co-CIPAAm)-grafted surfaces (CIPAAm; 1 mol % in feed) before and after RGDS immobilization after a 6-h culture without serum at 37 °C are readily evident.

Dissociation Control of Integrin−RGDS Specific Interactions. To control dissociation of specific interactions between cultured cell integrins and surface RGDS, spread HUVECs (1 day culture without serum at 37 °C) were exposed to the addition of soluble RGDS at 37 °C (Figure 4) and lower temperature treatment at 20 °C (Figure 5). Soluble RGDS (100 μM) spontaneously detaches HUVECs from RGDS−IC(X) based on competitive substitution of
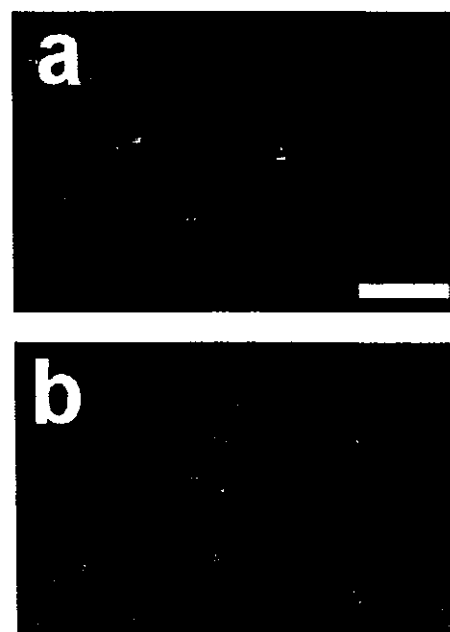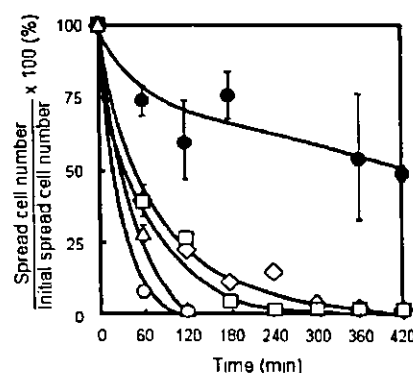
soluble RGDS for immobilized RGDS. Detachment rates depended on immobilized cell adhesive peptide densities represented by monomer carboxylate group composition in each feed. Moreover, detachment rates were accelerated dramatically by addition of higher concentrations of RGDS (data not shown). Low-temperature treatment at 20 °C also promoted cell detachment from RGDS−IC(X), where the detachment rate also decreased with increasing cell adhesive peptide surface content. Both treatments (addition of soluble RGDS at 20 °C) together accelerated cell detachment from RGDS−IC(5) over each separately (Figure 6).

To examine time-dependent cell-substrate interactions, HUVECs were cultured on RGDS−IC(1) for 4 h, 1 day, 3 days, and 7 days without serum at 37 °C and subjected to either addition or nonaddition of soluble RGDS at 37 or 20
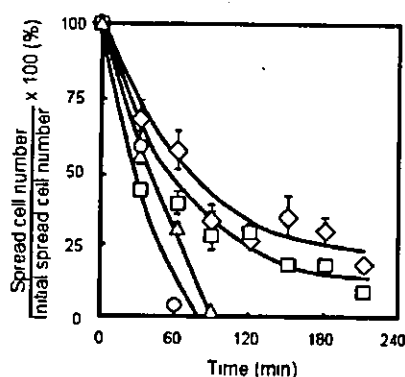
Figure 5. HUVEC detachment from RGDS-immobilized temperature-responsive culture surfaces by lowering the temperature. Cells on RGDS-IC(X) were subjected to low-temperature treatment at 20 °C after a 24-h culture at 37 °C without serum. CIPAAm compositions were 1 (open circle), 3 (triangle), 5 (square), and 10 mol % (diamond).
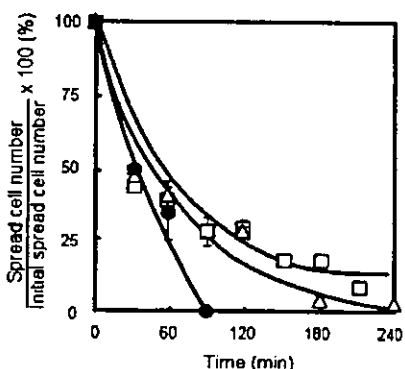

Figure 6. Comparison of the effects of soluble peptide addition and reduced culture temperature treatment on HUVEC detachment from RGDS-IC(5). Soluble RGDS (100 μM) was added into each culture dish after 24-h culture at 37 °C without serum, and these surfaces were incubated at 20 and 37 °C. Soluble RGDS (100 μM) addition (triangle), only temperature treatment at 20 °C (square), and temperature treatment at 20 °C with 100 μM of soluble RGDS (closed circle).

°C (Figure 7). Soluble RGDS addition became less effective with increasing culture time before each treatment (Figure 7a). With lower temperature treatment, detachment rates increased with increasing culture time (Figure 7b). Moreover, both treatments accelerated cell detachment from RGDS–IC(1), particularly after 1 and 3 day cultures (Figure 7c).

Discussion

Cell integrin ligand RGDS peptides covalently immobilized to temperature-responsive polymer grafted surfaces were assayed for cell attachment/detachment "on–off" control by culture temperature regulations. Polymer grafted amounts on the surface are approximately 2 μg/cm² estimated by attenuated total reflection Fourier transform infrared (ATR-FTIR) as described previously.[28] Carboxylate group densities on these surfaces calculated from the feed composition of CIPAAm were 0.2, 0.6, 1.0, and 2.0 nmol/cm² for RGDS(X)-IC(1), IC(3), IC(5), and IC(10), respectively. Hydrated shielding abilities of the polymers against ligands would depend on the relative size of the polymer chains to receptor active binding sites.[9] Changes in surface hydration,
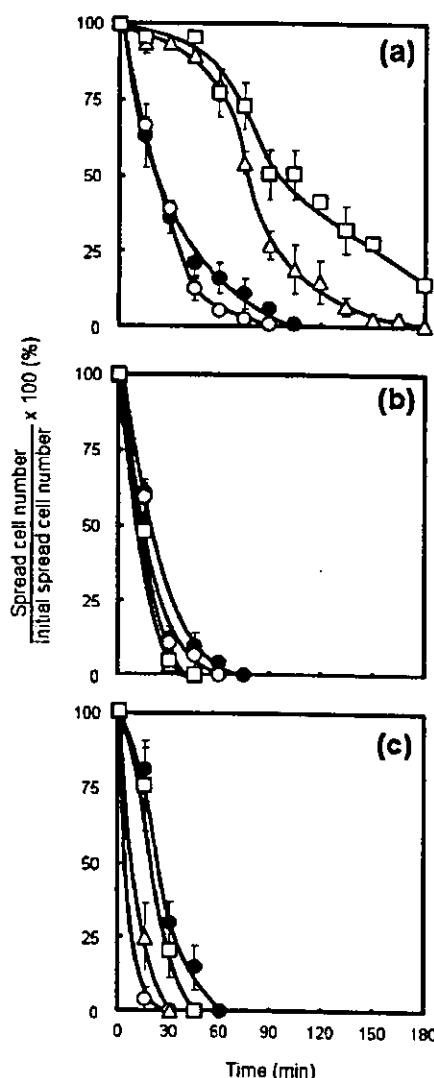

Figure 7. Effect of culture time of HUVECs on cell-substrate interaction. Cells seeded onto RGDS-IC(1) were cultured at 37 °C for 4 h (closed circle), 1 day (open circle), 3 day (triangle), and 7 days (square) and subjected to the following treatments: Soluble RGDS (100 μM) addition (a), only temperature treatment at 20 °C (b), and temperature treatment at 20 °C with 100 μM of soluble RGDS (c).

surface mechanical modulus, and support of spread cells in tension ("tensegrity")[30–34] would also depend on surface graft architecture, swelling below LCST, and less surface structural rigidity.

As seen in Figures 1–3, immobilization of RGDS on surfaces was critical for HUVEC spreading at 37 °C. RGDS enhanced integrin-mediated cell spreading, whereas the control tetrapeptide (RGES) did not (Figure 1), indicating recognition specificity. Healy et al. also showed that few or no focal contacts were formed by bone-derived cells on the RGE-immobilized surfaces and there was a significant difference between the adhesion strength of cells to RGD and RGE-immobilized surfaces.[35] Moreover, scant cell spreading was also observed for surfaces grafted with comonomer, AAc, in place of CIPAAm (Figure 2). Copolymerization of IPAAm with AAc shifts its LCST to a temperature higher than 37 °C,[36–38] and we have already

reported that P(IPAAm-*co*-CIPAAm) retains PIPAAm's thermal phase transition behavior because CIPAAm maintains a hydration environment around side chain groups essential to the phase transition.[26,39] We conclude, therefore, that low cell spreading on RGDS—IA(1) is attributed to highly hydrated, unreacted acrylic acid carboxyl groups distinct from CIPAAm surfaces.

HUVEC detachment behavior from RGD-IC(X) by reducing the temperature below the polymer LCST depended upon the immobilized RGDS content (Figure 5). This behavior was very analogous to that produced by soluble RGDS addition (Figure 4). Although HUVECs cultured in FBS on TCPS resisted detachment by soluble RGDS addition, all spread cells detached from RGDS—IC(X) consistent with respective immobilized RGDS amounts. This mechanism is explained by competitive ligand—receptor binding affinity changes, where substitution of the soluble RGDS ligand for immobilized RGDS occurs readily on lower peptide density surfaces such as RGDS—IC(1). HUVEC detachment by reducing the temperature is also explained by a decreasing association between cell integrins and the RGDS by surface swelling and loss of cell tension on hydrated polymer grafted chains. It is not likely that low temperature treatment directly causes integrin-RGDS dissociation because it is well-known that cell—matrix binding is retained even at 4 °C.[40] Mrksich et al. pointed out that available ligand densities for binding cellular receptors depended on ligand conditions because the adsorbed ligand distribution, conformation, and orientation were changed by the choice of substrates.[41] It is plausible that only slight microenvironmental changes of immobilized ligands caused by temperature-dependent swelling of ligand-attached polymer chains reduces surface rigidity upon which adherent cells are attached. Because these spread cells are in tension, a sudden loss of this tension and traction prompts detachment and rounding. Cell receptor—ligand occupancy is a function of surface cell spreading and tension: when hydrated and softened, the polymers promote ligand—receptor dissociation. This result is similar to the competitive detachment assay by soluble RGDS addition. Accelerated cell detachment behavior in Figure 6 suggests possible additivity of soluble RGDS addition and low temperature treatment that drastically dissociate the receptor from the ligand.

The cell—substrate interaction occurs in a series of steps beginning with sufficient minimal integrin-mediated binding, followed by increasing receptor recruitment, cell polarization, and cytoskeletal and cytoplasmic reorganization.[42] Cells alter the formation of adhesive contacts with the substrate, including receptor clusters and focal contact adhesion, in a time-dependent manner.[43,44] Therefore, we propose that HUVECs change their interactions with RGDS—IC(X) as a function of culture time before cell detachment assay. Large differences in the effects of soluble RGDS addition on cell detachment are observed between 1 day and 3 day cultures at 37 °C (Figure 7a). Delayed cell detachment after a 3 day (or 7 day) culture is attributed to additional interactions developing between cells and surfaces including extracellular matrix production, remodeling, and nonspecific interactions. Hence, with increasing time, cells resist surface removal even

if the specific, original integrin-mediated ligand interactions dissociate. Although slower with culture time, all cells detach eventually because loss of cell tension by the dissociation of integrin-RGDS binding likely triggers several signal transduction mechanisms for cytoskeletal changes, rounding, and dissociation of other interactions with the substrate. In contrast, the detachment rates of cells by reducing the temperature increases with increasing culture time because long-term culture increases nonspecific cell—surface interactions (lower affinity than specific integrin—RGDS interactions) but are all induced to release by grafted polymer swelling surface softening and low cell tension on the surface (Figure 7b). Both treatments (lowering the temperature and soluble RGDS addition) resulted in acceleration of cell detachment, but degrees of acceleration were slight because in this system low temperature treatments more effectively produce cell detachment compared with soluble RGDS addition at this concentration (100 μM).

In conclusion, RGDS-immobilized temperature-responsive polymer-grafted surfaces promote the HUVEC adhesion and spreading by their biospecific activity in serum-free media. At temperatures below the grafted polymer's LCST, integrin—RGDS association decreases due to loss of cell tension and surface anchoring, prompting cells to round and then detach. Observed "on—off" control of specific integrin-RGDS binding only by temperature regulation is very important for cell function regulation because cell surface integrins not only bind to cell adhesive ligands in ECM but also serve to produce subsequent cell signal transduction activity. Moreover, this approach facilitates a serum-free cell culture for the safety of clinical applications using cultured cells and noninvasive cell recovery (no enzymes) that help maintaining original cell function, both important to applications of tissue engineering.

References and Notes

(1) Whitesides, G. M.; Mathias, J. P.; Seto, C. T. *Science* **1991**, *254*, 1312—1319.

(2) Irvine, D. J.; Mayes, A. M.; Griffith, L. G. *Biomacromolecules* **2001**, *2*, 85—94.

(3) Yamato, M.; Kwon, O. H.; Hirose, M.; Kikuchi, A.; Okano, T. *J. Biomed. Mater. Res. Short Commun.* **2001**, *55*, 137—140.

(4) Fong, R. B.; Ding, Z.; Long, C. J.; Hoffman, A. S.; Stayton, P. S. *Bioconjugate Chem.* **1999**, *10*, 720—725.

(5) Schlosser, M.; Hahmann, J.; Ziegler, B.; Augstein, P.; Ziegler, M. *J. Immunoassay* **1997**, *18*, 289—307.

(6) Kumar, A.; Kamihira, M.; Galaev, I. Y.; Mattiasson, B.; Iijima, S. *Biotechnol. Bioeng.* **2001**, *75*, 570—580.

(7) Tang, A.; Wang, C.; Stewart, R. J.; Kopecek, J. *J. Controlled Release* **2001**, *72*, 57—70.

(8) Kurisawa, M.; Yokoyama, M.; Okano, T. *J. Controlled Release* **2000**, *69*, 127—137.

(9) Ding, Z.; Fong, R. B.; Long, C. J.; Stayton, P. S.; Hoffman, A. S. *Nature* **2001**, *411*, 59—62.

(10) Yoshizako, M.; Akiyama, Y.; Yamanaka, H.; Shinohara, Y.; Hasegawa, Y.; Carredano, Enrique.; Kikuchi, A.; Okano, T. *Anal. Chem.* **2002**, *74*, 4160−4166.

(11) Hynes, R. O. *Cell* **1992**, *69*, 11−25.

(12) Miyamoto, S.; Akiyama, S. K.; Yamada, K. M. *Science* **1995**, *267*, 883−885.

(13) Chicurel, M. E.; Chen, C. S.; Ingber, D. E. *Curr. Opin. Cell Biol.* **1998**, *10*, 232−239.

(14) Grinnell, F. *Trends Cell Biol.* **2000**, *10*, 362−365.

(15) Grinnell, F. *Int. Rev. Cytol.* **1978**, *53*, 65−144.

(16) Piershbacher M. D.; Rouslahti E. *Proc. Natl. Acad. Sci. U.S.A.* **1984**, *81*, 5985−5988.

(17) Yamada, K. M. *J. Biol. Chem.* **1991**, *266*, 12809−12812.

(18) Massia, S.; Hubbell, J. A. *J. Cell. Biol.* **1991**, *114*, 1089−1100.

(19) Houseman, B. T.; Mrksich, M. *Biomaterials* **2001**, *22*, 943−955.

(20) Maheshwari, G.; Brown, G.; Lauffenburger, D. A.; Wells, A.; Griffith, L. G. *J. Cell Sci.* **2000**, *113*, 1677−1686.

(21) Stile, R. A.; Healy, K. E. *Biomacromolecules* **2001**, *2*, 185−194.

(22) Rezania, A.; Healy, K. E. *J. Biomed. Mater. Res.* **2000**, *52*, 595−600.

(23) Garcia, A. J.; Keselowsky, B. G. *Crit. Rev. Eukaryot. Gene Expr.* **2002**, *52*, 151−162.

(24) Saneinejad, S.; Shoichet, M. S. *J. Biomed. Mater. Res.* **1998**, *42*, 13−19.

(25) Tong, Y. W.; Shoichet, M. S. *J. Biomater. Sci. Polym. Ed.* **1998**, *9*, 713−729.

(26) Aoyagi, T.; Ebara, M.; Sakai, K.; Sakurai, Y.; Okano, T. *J. Biomater. Sci. Polym. Ed.* **2000**, *11*, 101−110.

(27) Kikuchi, A.; Okuhara, M.; Karikusa, F.; Sakurai.; Okano, T. *J. Biomater. Sci. Polym. Ed.* **1998**, *9*, 1331−1348.

(28) Ebara M.; Yamato, M.; Hirose, M.; Aoyagi T.; Sakai K.; Okano T. *Biomacromolecules* **2003**, *4*, 344−349.

(29) Hautanen, A.; Gailit, J.; Mann, D. M.; Ruoslahti, E. *J. Biol. Chem.* **1989**, *264*, 1437−1442.

(30) Chicurel, M. E.; Chen, C. S.; Ingber, D. E. *Curr. Opin. Cell Biol.* **1998**, *10*, 232−239.

(31) Ingber, D. E. *Annu. Rev. Physiol.* **1997**, *59*, 575−599.

(32) Ingber, D. E.; Dike, L.; Hansen, L.; Karp, S.; Liley, H.; Maniotis, A.; McNamee, H.; Mooney, D.; Plopper, G.; Sims, J. *Int. Rev. Cytol.* **1994**, *150*, 173−224.

(33) Ingber, D. E. *Cell* **1993**, *75*, 1249−1252.

(34) Ingber, D. E. *J. Cell Sci.* **1993**, *104*, 613−27.

(35) Rezania, A.; Thomas, C. H.; Branger, A. B.; Waters, C. M.; Healy, K. E. *J. Biomed. Mater. Res.* **1997**, *37*, 9−19.

(36) Feil, H.; Bae, Y. H.; Feijen, J.; Kim, S. W. *Macromolecules* **1993**, *26*, 2496−2500.

(37) Kaneko, Y.; Nakamura, S.; Sakai, K.; Aoyagi, T.; Kikuchi, A.; Sakurai, Y.; Okano, T. *Macromolecules* **1998**, *31*, 6099−6105.

(38) Yu, H.; Grainger, D. W. *J. Appl. Polym. Sci.* **1993**, *49*, 1553−1563.

(39) Ebara, M.; Aoyagi, T.; Sakai, K.; Okano, T. *Macromolecules* **2000**, *33*, 8312−8316.

(40) Grinnell, F.; Lang, B. S. *J. Cell. Biol.* **1981**, *87*, p127a.

(41) Mrksich, M. *Chem. Soc. Rev.* **2000**, *29*, 267−273.

(42) Benjamin, G.; Bershadsky, A.; Pankov, R.; Yamada, K. M. *Nat. Rev.* **2001**, *2*, 793−805.

(43) Baneyx, G.; Baugh, L.; Vogel, V. *Proc. Natl. Acad. Sci. U.S.A.* **2002**, *99*, 5139−5143.

(44) Dejana, E.; Colella, S.; Conforti, G.; Abbadini, M.; Gaboli, M.; Marchisio, P. C. *J. Cell. Biol.* **1988**, *107*, 1215−1223.

BM0343601

Scientific Discovery

Most of the papers in this section are studies of cellular biology in urological cancer. Each of the four papers assess a particular aspect of four different types of cancer: prostate, bladder, renal, and testicular. The other two reports are on unrelated issues; in the first, the authors write about urothelial regeneration using viable cultured urothelial cell sheets grafted onto demucosalized gastric flaps, and in the second, on the *in vivo* expression of nitric oxide synthase.

Urothelium regeneration using viable cultured urothelial cell sheets grafted on demucosalized gastric flaps

Y. SHIROYANAGI*†, M. YAMATO*†, Y. YAMAZAKI†, H. TOMA† and T. OKANO*†
*Institute of Advanced Biomedical Engineering and Science and †Department of Urology, Tokyo Women's Medical University, and †CREST, Japan Science and Technology Corporation, Tokyo, Japan

OBJECTIVE

To evaluate urothelium regeneration by grafting viable cultured urothelial cell sheets, harvested from temperature-responsive culture surfaces, on demucosalized gastric flaps in a dog model.

MATERIALS AND METHODS

Viable urothelium was obtained from eight beagle dogs by partial cystectomy. Harvested urothelial cells were seeded on temperature-responsive culture dishes modified with the thermally sensitive polymer, poly(N-isopropylacrylamide). Urothelial cells cultured for 3 weeks generated contiguous urothelial cell sheets that were noninvasively harvested with no enzymatic treatment from these dishes, by reducing culture temperature. Urothelial cell sheets were autografted onto surgically demucosalized gastric flaps. Three weeks after autografting the dogs were killed and the gastric flaps with the urothelial cell sheets were examined. Cell and tissue characteristics were compared between these urothelial cell sheet-grafted gastric flaps and native urothelium. Ultrafine structures were also examined by electron microscopy.

RESULTS

Five of the eight urothelial cell sheet-grafted flaps showed viable urothelial regeneration.

Urothelial cell sheets attached spontaneously to demucosalized tissue surfaces completely, with no suture or fixing, and developed into a stratified viable epithelium very similar to native urothelium. Regenerated urothelium remained unstained by antiproton pump antibody, which typically stains epithelial cells positively in gastric mucosal layers. On three of the eight flaps where there were severe haematomas, grafted cell sheets were not adherent and there was no urothelial regeneration.

CONCLUSION

Urothelial cell sheets were autografted onto dog demucosalized gastric flaps successfully, with no suture or fixation, generating a multilayered urothelium *in vivo*. The novel intact cell-sheet grafting method rapidly produces native-like epithelium *in vivo*. This versatile technology should prove useful in urinary tract tissue engineering and surgical reconstruction.

KEYWORDS

urothelium, cell sheet engineering, temperature-responsive culture surfaces, autologous transplantation, bladder augmentation, tissue regeneration
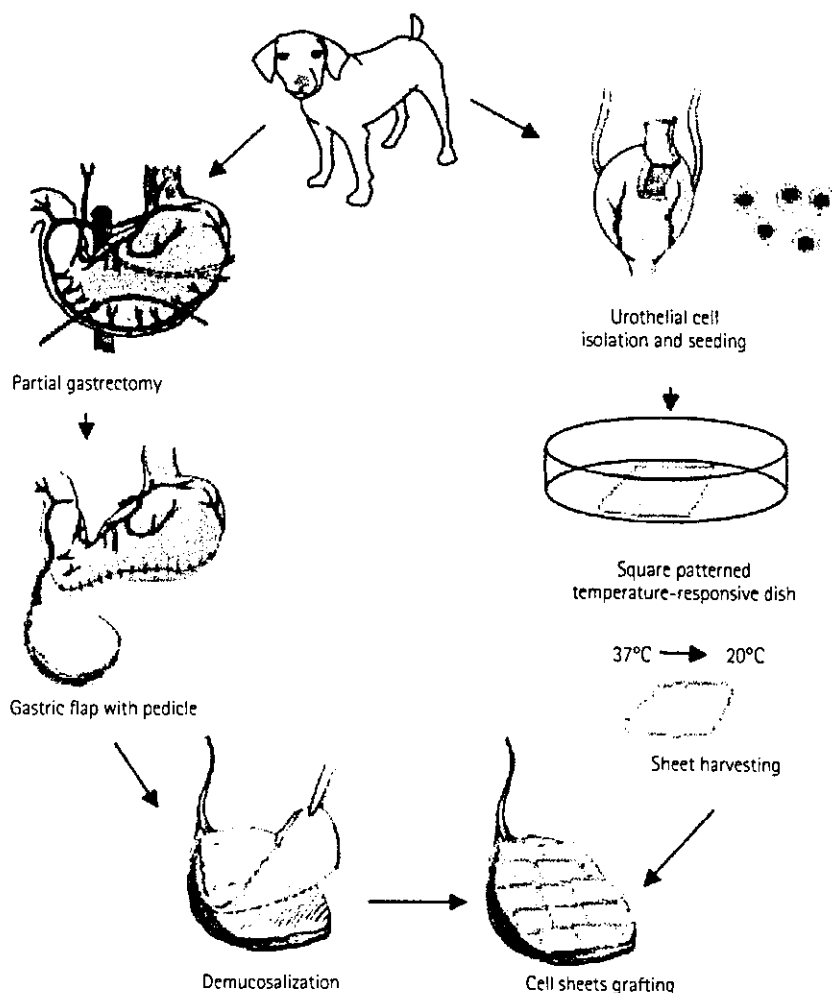
-413-

Bladder reconstruction has an increasingly important role in the treatment of adult and paediatric patients after bladder resection for malignancy, or with low-compliance, low-capacity bladders. The indications for urinary diversion and reconstruction using intestinal segments have expanded greatly. However, gastrointestinal mucosa often causes various complications, including electrolyte imbalance, stone formation, UTI and mucus production [1,2]. To solve these complications some investigators have attempted to cover the demucosalized intestinal surface with urothelial grafts obtained from the bladder mucosa or cultured urothelium [3-5].

Previous work in our laboratory showed that various intact cell sheets from diverse primary sources, including urothelium, can be harvested intact with no enzymatic proteolysis (e.g. trypsin or dispase digestion), by using temperature-responsive culture systems [6-8]. In the present study native gastrointestinal mucosa was replaced with cultured urothelial cell sheets harvested noninvasively from temperature-responsive culture surfaces in a surgical dog model of reconstruction. The purposes of this study were; (i) to investigate the utility of direct grafting of cultured urothelial cell sheets transplanted onto demucosalized gastric flaps, and (ii) to examine the histology of urothelial regeneration on the gastrointestinal stromal layer.

All experimental protocols were approved by the animal welfare committee of Tokyo Women's Medical University (Approval no. 02-55, 2002). The experimental scheme is shown in Fig. 1; nine dogs underwent the procedures under general anaesthesia. Eight adult beagle dogs (10-12 kg, 1 year old, female) first had a partial cystectomy to obtain urothelial cells, and these primary urothelial cells were seeded on temperature-responsive culture dishes. Three weeks later the same dogs were re-anaesthetized and a segment of stomach isolated and demucosalized. Cultured urothelial cell sheets were autografted onto exposed gastric submucosal layers of surgically constructed flaps by simple topical placement with no sutures or fixation, but the flap was placed within a protective latex pouch to prevent

FIG. 1. Scheme for the urothelial cell sheet autografting experiment. Canine urothelial cells were isolated and cultured on temperature-responsive culture dishes. The urothelial cell sheets, noninvasively harvested by reducing culture temperature after 3 weeks, were autografted onto a canine demucosalized gastric flap surgical model.

Partial gastrectomy

Gastric flap with pedicle

Demucosalization

Urothelial cell isolation and seeding

Square patterned temperature-responsive dish

37°C ➡ 20°C

Sheet harvesting

Cell sheets grafting

abdominal adhesion, and returned to the abdominal cavity. After a further 3 weeks all dogs were killed and the transplanted flaps excised and examined. In one dog (a control) no cell sheet was grafted during identical surgery.

For anaesthesia the dogs were premedicated with 0.04 mg/kg atropine and 15 mg/kg ketamine intramuscularly, and then given 15 mg/kg thiopental sodium. An endotracheal tube was then placed and anaesthesia maintained using halothane and nitrous oxide.

For urothelial cell sheet preparation, a laparotomy was made via midline incision and

a 2.0 × 2.0 cm area was excised from the dome of the bladder. The bladder was closed in one layer. Both urothelium and submucosal layers were stripped from the smooth muscle layer and treated with 1000 U/mL dispase (Godoshusei, Tokyo, Japan). After this enzymatic treatment the epithelial layer was peeled from the stromal layer and digested in 0.1% trypsin/0.04% EDTA to obtain a single-cell suspension. Then $1-2 \times 10^5/cm^2$ dissociated urothelial cells were seeded onto square-patterned temperature-responsive cultured dishes and cultured according to the method of Rheinwald and Green [9,10] with a feeder layer of mitomycin C-treated NIH 3T3 cells. The culture medium was Ham's F-12 medium/DMEM in a 1 : 3 ratio supplemented

FIG. 2. Urothelial cell sheets and demucosalized gastric flaps. Macroscopic view of square-patterned urothelial cell sheets harvested by reducing culture temperature. Without substrate support, the sheet will respond to internal cell stresses to deform plastically over time after release, (a). H&E staining of the urothelial cell sheet shows multilayers of cultured urothelial cells in sheets, (b). Anti-uroplakin antibody staining along the apical surface of the urothelial cell sheets, (c). Macroscopic view of the demucosalized gastric flaps, (d). Scale bar represents 1 cm in (a) and (d), and 100 μm in (b) and (c), respectively.
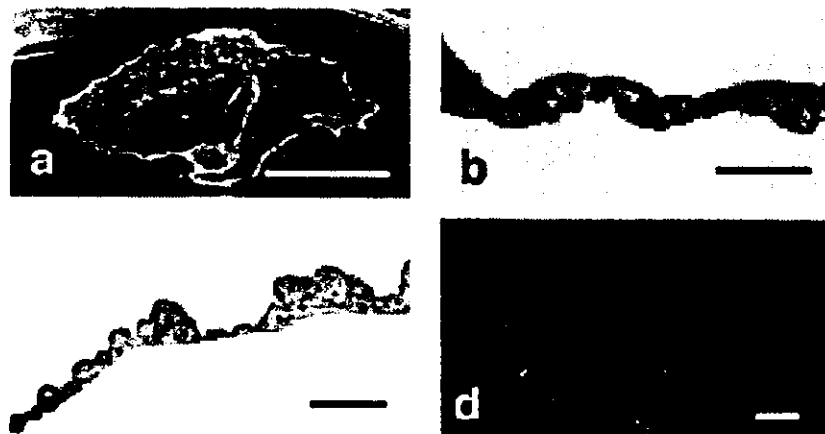
with 5% fetal bovine serum, insulin (5.0 μg/mL), transferrin (5.0 μg/mL), triiodothironine (2 nmol/L), cholera toxin (1 nmol/L), hydrocortisone (0.4 μg/mL), recombinant human epidermal growth factor (Gibco BRL Life Technologies, Grand Island, NY, 10 ng/mL), recombinant fibroblast growth factor-7 (R&D Systems, Inc., Minneapolis, MN, 10 ng/mL), penicillin and streptomycin. Three weeks later the dishes were incubated at 20 °C for 30 min to yield contiguous, intact urothelial cell sheets free from the culture substrate, floating in media (Fig. 2a). These sheets were transferred immediately *in vivo* to tissue surfaces.

For the autografts of urothelial cell sheets onto demucosalized gastric flaps, 3 weeks after initial bladder excision the same eight dogs were re-anaesthetized. Through a midline incision a 5-7 cm segment of the greater curvature of stomach was isolated using a Proximate Linear Cutter™ (Ethicon Endo-Surgery, Cincinnati, OH), leaving the gastric segment with its vascular pedicle intact. The mucosa of the isolated gastric segment was then mechanically stripped off with scissors. The surface of the demucosalized gastric flap was cauterized for haemostasis. Urothelial cell sheets harvested from the culture dishes were carefully removed from the dishes and then placed topically directly onto demucosalized gastric flap areas with no fixation. The urothelial cell

sheets were transferred with a small transparency sheet because they were too fragile to manipulate with forceps. The flap was then placed in a latex pouch to prevent adhesion and returned to the abdominal cavity.

Standard tissue sections were examined after haematoxylin and eosin (H&E) staining and periodic acid/Schiff reaction. For immunohistochemistry the sections were pretreated with proteinase K (Dako, Denmark), washed in Dulbecco's PBS and blocked with 1% BSA solution. The sections were then incubated with diluted primary antibodies; mouse monoclonal antihuman cytokeratin, AE1/AE3 (Dako), mouse monoclonal antihuman cytokeratin 7, OV-TL 12/30 (Dako), and rabbit antiserum to total bovine uroplakins (kindly provided by Dr T.T. Sun, New York University, NY), rinsed with PBS, and incubated with horseradish peroxidase-conjugated secondary antibody (LASB kit, Dako). Sections were developed with diaminobenzidine and counterstained with haematoxylin. Frozen tissue sections of the grafts were cut at 10 μm, mounted on glass slides and fixed at room temperature with 4% paraformaldehyde in PBS for 20 min. They were then washed with PBS, permeabilized with 0.5% Triton X-100 in PBS for 5 min, washed three times with PBS, and blocked with 0.1% BSA in PBS for 2 h. Primary antibodies used were antiheparan sulphate

proteoglycans, A7L6 (Chemicon International, CA, USA), rabbit polyclonal antihuman placental type IV collagen, 10760 (Progen Biotechnik, Heidelberg, Germany) and antiproton pump, 1H9 (Medical & Biological Laboratories, Nagoya, Japan). Sections were incubated with the primary antibodies for 24 h, rinsed with PBS three times and incubated for 2 h with the secondary fluorescein isothiocyanate-conjugated goat anti-IgG antibody (Cappel Products, Aurora, OH, USA).

For electron microscopy, tissue samples were embedded in Quetal 812 (Nisshin, Tokyo, Japan) and ultrathin sections (90 nm) were cut on an ultramicrotome, and then stained with uranyl acetate and lead citrate. The sections were examined at 80 kV using a transmission electron microscope. Other samples were cut into small pieces, fixed in 2.5% glutaraldehyde for 1 h, postfixed in 1.5% osmium tetroxide, dehydrated through graded alcohols, dried with the *t*-butyl alcohol method and osmium-sputtered for 15 s [11]. These samples were examined using a scanning electron microscope.

RESULTS

Square urothelial cell sheets were reliably obtained (Fig. 2a), and consisted of one to four cell layers (Fig. 2b), staining positively with antiuroplakin antibodies (Fig. 2c). The haemorrhage of the demucosalized gastric flap surface was controlled and a thin fibrin layer was found on the surface (Fig. 2d).

None of the nine dogs that underwent surgery died afterward. All demucosalized gastric flaps with and with no cell sheet treatment appeared to be smaller and thicker than the originals at death. There was no gastric mucosal re-growth in the control dog (Fig. 3a). Of the eight dogs with a urothelial cell sheet autograft, five had viable regenerated epithelium (Fig. 3f-j); there was urothelial regeneration on almost all the surface of the grafted gastric flaps. Urothelial cells migrated and covered the small gaps between grafted cell sheets. The morphological structures of the regenerated epithelium on the demucosalized gastric flaps were very similar to native urothelium (Fig. 3b-e), except for the superficial cell layer. There was a squamous change in the superficial layer, and neither gland nor mucous granule morphology in any site of the

-415-

FIG. 3. Histological characterization. Control demucosalized gastric graft (noncell sheet treated), (a). Native urothelium of canine ureter, (b-e). regenerated urothelium on a demucosalized gastric flap, (f-j). H&E staining (a,b,f). Periodic acid/Schiff reaction showed no observable mucous granules, (g). There was no gastric mucosal re-growth on the control graft, (a). Regenerated urothelium expresses pan-cytokeratin similarly to that observed for native urothelium, (c,h). The expression of cytokeratin 7 is strong in native urothelium and weak in the regenerated urothelium, (d,i). The regenerated urothelium does not express uroplakin but it is well-expressed in native urothelium, (e,j). Scale bar represents 100 μm.
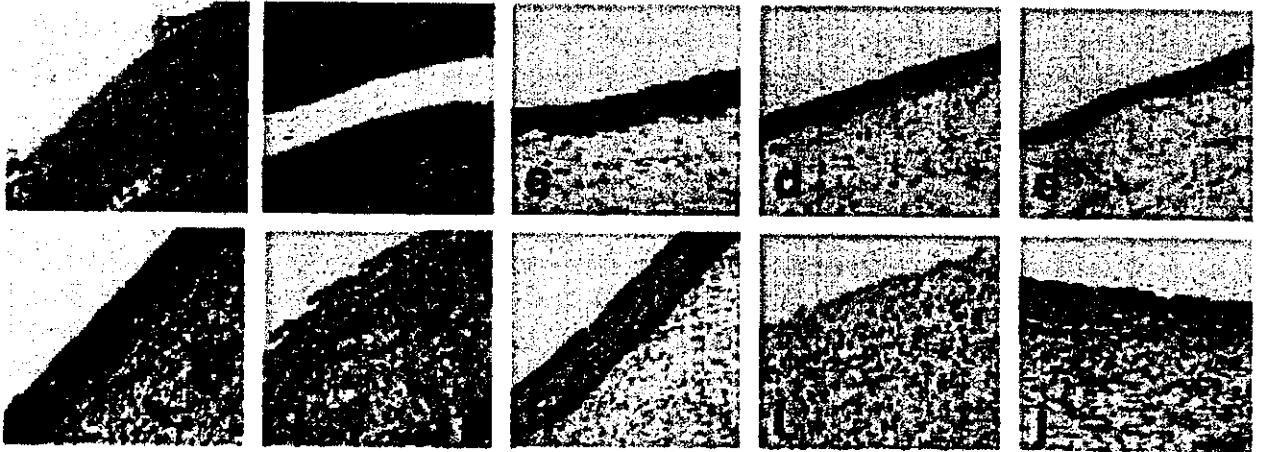
regenerated urothelium (Fig. 3g). Subepithelial tissue was moderately infiltrated with mononuclear cells and showed substantial neovascularization. Urothelium was not regenerated on three of eight flaps where there were severe haematomas.

All layers of regenerated urothelium stained positively with anticytokeratin antibody, similarly to native urothelium (Fig. 3c,h). Cytokeratin 7 was well-expressed in superficial and intermediate cell layers of native urothelium (Fig. 3d), but stained only faintly in regenerated epithelium (Fig. 3i). Uroplakins were strongly expressed in the superficial umbrella cells of native urothelium (Fig. 3e), but were not present in regenerated epithelium (Fig. 3j).
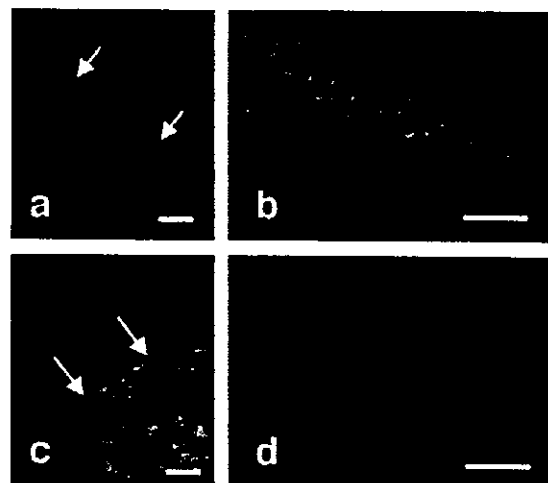

FIG. 4.
Immunofluorescence microscopy. The basement membrane (arrow) is positively stained with antiheparan sulphate proteoglycan antibody in native urothelium (a) and in regenerated urothelium (c). The basement membrane of blood vessels was also stained. Note the considerable evidence for revascularization in gastric flaps with regenerated epithelium (c). The proton pump was well-expressed in gastric glands (b), but not in regenerated epithelium (d). Scale bar represents 100 μm.

Heparan sulphate proteoglycan, a typical component of basement membrane, was deposited along the border between regenerated epithelial cell layers and gastric submucosal layers (Fig. 4c), as well as the basal side of the native urothelium (Fig. 4a). Basement membrane from blood vessels was also stained with antibody in both native bladder and gastric flaps with regenerated epithelium. There was more vascularization in the submucosal layer with regenerated epithelium than in the native gastric submucosal layer (data not shown). Basement membrane in regenerated urothelium was also stained with anticollagen IV antibody,

similarly to native urothelium (data not shown). Proton pump (H⁺, K⁺-ATPase), essential to produce gastric acid, was well-expressed in native gastric mucosa (Fig. 4b), but was not in regenerated epithelium (Fig. 4d).

Transmission electron microscopy showed that superficial cells of native urothelium contained numerous cytoplasmic vesicles (Fig. 5a). However, those of the regenerated epithelium had fewer cytoplasmic vesicles and abundant microfilaments (Fig. 5c). Scanning electron microscopy showed the 'cobble-stone' appearance characteristic of

native urothelium (Fig. 5b) in the regenerated epithelium (Fig. 5d). However, in regenerated epithelium, the apical cells were smaller than those of native urothelium. Furthermore, native apical cells were flat with tightly connected cell-to-cell borders (Fig. 5b). In contrast, the regenerated apical cells were slightly rounded and each cell appeared isolated (Fig. 5d).

DISCUSSION

In the last decade, many procedures have been examined to solve the complications of

1072

FIG. 5. *Scanning and transmission electron microscopy. Native urothelium (a, b) and regenerated urothelium (c, d). (a) and (c) are transmission and (b) and (d) are scanning. Scale bar represents 10 μm.*
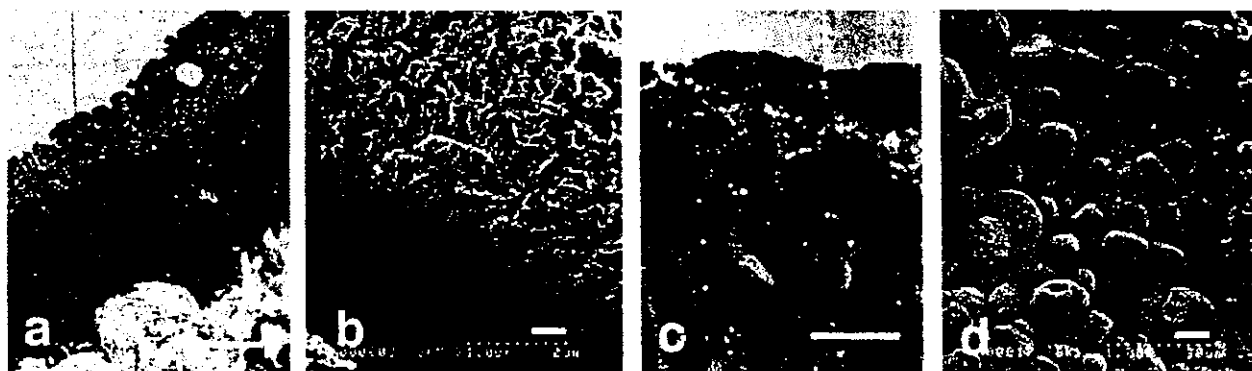
bladder reconstructions using gastrointestinal segments. Gonzalez *et al.* [12] reported a reconstruction technique using seromuscular colocystoplasty lined with urothelium. The seromuscular colonic segment was placed over the urothelial 'bubble' of the bladder the detrusor of which was lifted off the urothelium. Recent advances in tissue-engineering techniques would also potentially allow various new methods of urinary bladder reconstruction, to avoid clinical complications of reconstruction using gastrointestinal flaps [13–15]. However, these approaches have not yet matured for clinical use, for several technical reasons. Meanwhile, covering demucosalized intestinal surface with urothelium grafts obtained from the bladder mucosa or cultured urothelium has been attempted [3–5]. Merguerian *et al.* [3] grafted cultured urothelial cells grown on a biodegradable scaffold onto the demucosalized bowel segment in the rabbit. However, the grafted cells failed to regenerate urothelium. Schaefer *et al.* [4] achieved regenerated urothelium by transplanting cultured urothelium on collagen membranes onto demucosalized gastrointestinal seromuscular segments.

In the present study, cultured canine urothelial cell sheets were grafted successfully onto demucosalized gastric flaps, and a multilayered epithelium regenerated *in vivo*. Aktug *et al.* [5] reported that prefabricated seromuscular flaps partially grafted with urothelium (with no culture) before augmentation cystoplasty helped to avoid the complications caused by intestinal mucosa, and resulted in good bladder capacity. In their method the bladder must be fully opened to obtain large urothelial

samples. Cilento *et al.* [16] estimated that it would be theoretically possible to expand a urothelial strain from a single specimen that initially covers a surface area of 1 cm^2 to one covering a surface area of 4202 m^2 within 8 weeks. Using their method of cell culture and our cell-sheet harvesting technology, there is no need to open the bladder for primary culture of urothelium, when small pieces of urothelium can be readily harvested by endoscopy and expanded *in vitro* to cover large seromuscular flaps. If urothelium is taken from the renal pelvis, the engineered flap grafted with cultured urothelial cell sheets can be obtained with no need for bladder biopsy. This is a benefit not only for bladder augmentation but also for whole bladder reconstruction in patients whose bladder must be resected.

Previous work in our laboratory showed that various intact cell sheets from diverse primary sources can be harvested intact with no enzymatic proteolysis (e.g. trypsin or dispase digestion) by using temperature-responsive culture systems [6–8]. To prepare the dish a temperature-responsive polymer, poly(N-isopropylacrylamide), is bonded as a thin overlayer onto commercially available culture dish surfaces using electron beam irradiation [17,18]. This surface is slightly hydrophobic in culture at 37 °C, culturing seeded cells normally, and hydrating spontaneously below 32 °C to become hydrophilic [17,18]. At this reduced temperature, cultured adherent cells spontaneously detach from the rapidly hydrating surface as a single contiguous sheet. Importantly, multilayered or even patterned viable tissue-like cell sheet constructs can be fabricated and transplanted

in numerous tissue-regeneration models [19,20].

Urothelial cell sheets were noninvasively harvested by using temperature-responsive culture dishes; proteolytic enzymes (e.g. trypsin or dispase) typically required for cell culture but often destructive to cultured cells can be eliminated [6]. We previously reported that cell-cell junction proteins and extracellular matrix, e.g. cadherin, fibronectin, and laminin, remain intact during such cell-sheet harvest with no enzymes [6–8,21]. These intact cell adhesive proteins facilitate direct, rapid cell-sheet attachment on the demucosalized gastric flap surface. Furthermore, this cell sheet technology has the significant advantage that neither synthetic scaffold nor delivery vehicle is needed to graft the cultured cells *in vivo*. Various delivery vehicles, including collagen sponges, fibrin glue and synthetic biodegradable polymers, have been reported with varying success rates [3,22–24]. A cell-delivery vehicle should have several critical features, including biocompatibility, well-controlled biodegradation, benign cytotoxicity, high affinity for biological integration, and reduced potential for infection. These features are often difficult to obtain. Indeed, cell therapies have limited clinical surgical utility to date, particularly in urological applications. Therefore, the present method which requires no vehicle is better.

Urothelial cell sheets expressed characteristic urothelial uroplakins, while regenerated urothelium on demucosalized gastric flaps did not. Uroplakins are specific molecular markers of the asymmetric unit membrane of urothelium [25]. The structure of the

1073